

Article

Integrated Morpho-Bathymetric, Seismic-Stratigraphic, and Sedimentological Data on the Dohrn Canyon (Naples Bay, Southern Tyrrhenian Sea): Relationships with Volcanism and Tectonics

Gemma Aiello ^{*}, Marina Iorio , Flavia Molisso and Marco Sacchi 

Istituto di Scienze Marine (ISMAR), Consiglio Nazionale delle Ricerche (CNR), Sezione Secondaria di Napoli, 80133 Napoli, Italy; marina.iorio@iamc.cnr.it (M.I.); flavia.molisso@cnr.it (F.M.); marco.sacchi@cnr.it (M.S.)

* Correspondence: gemmaiello@virgilio.it or gemma.aiello@cnr.it; Tel.: +39-81-8960050 or +39-81-5423820

Received: 14 May 2020; Accepted: 12 August 2020; Published: 17 August 2020



Abstract: Submarine canyons are geomorphologic lineaments engraving the slope/outer shelf of continental margins. These features are often associated with significant geologic hazard when they develop close to densely populated coastal zones. The seafloor of Naples Bay is deeply cut by two incisions characterized by a dense network of gullies, namely the Dohrn and Magnaghi canyons, which develop from the shelf break of the Campania margin, down to the peripheral rise of the Eastern Tyrrhenian bathyal plain. Seismic-stratigraphic interpretation of multichannel seismic reflection profiles has shown that quaternary tectonics and recent to active volcanism have exerted a significant control on the morphological evolution and source-to sink depositional processes of the Dohrn and Magnaghi submarine canyons. The Dohrn canyon is characterized by relatively steep walls hundreds of meters high, which incise a Middle-Late Pleistocene prograding wedge, formed by clastic and volcanoclastic deposits associated with the paleo-Sarno river system during the Mid-Late Pleistocene. The formation of the Dohrn canyon predates the onset of the volcanic eruption of the Neapolitan Yellow Tuff (NYT), an ignimbrite deposit of ca. 15 ka that represents the bedrock on which the town of Napoli is built. Integrated stratigraphic analysis of high-resolution seismic profiles and marine gravity core data (C74_12) collected along the flanks of the eastern bifurcation of the head of Dohrn Canyon suggests that depositional processes along the canyon flanks are dominated by gravity flows (e.g., fine-grained turbidites, debris flows) and sediment mass transport associated with slope instability and failure.

Keywords: submarine canyon; mass transport; volcanic activity; Gulf of Naples

1. Introduction

The continental slope and outer shelf of the Naples Bay are deeply cut by two submarine incisions—the Dohrn and the Magnaghi canyons—that form a large drainage system of this coastal marine area during the Late Quaternary. The Bay is located on the Eastern margin of the Tyrrhenian Sea, a Neogene-Quaternary extensional domain that includes small areas floored with oceanic-type crust. The Tyrrhenian Sea encompasses a number of peripheral (“peri-Tyrrhenian”) basins, along its borders, like Naples Bay [1–4], that exhibit remarkable differences in size, thickness, and stratigraphic architecture.

Canyons and gullies are major components of continental slope morphology, as they represent a critical link between coastal waters and abyssal depths, by transferring sediments, nutrients and even litter and pollutants into deep-water settings. The aim of this research is to provide a contribution toward the understanding of depositional and erosional processes along a major canyon system developing on a tectonically active continental margin, associated with active volcanism, during the

interplay of Late Quaternary–relative sea-level oscillations [5–14]. Active volcanic districts along the coasts of the Naples Bay are represented by Somma-Vesuvius and Campi Flegrei, including Ischia and Procida Islands.

The volcanic district of Campi Flegrei has been active since at least ~60 ka BP, mostly with explosive eruptions. The area has been interpreted as the result of two large caldera collapses related to the eruptions of the Campanian Ignimbrite (~39 ka) [15–29] and the Neapolitan Yellow Tuff (NYT, ~15 ka). The southern submerged margin of the Campi Flegrei caldera is represented by the Pozzuoli Bay [28,30–33].

Somma-Vesuvius is a stratovolcano with alternating pyroclastic and lava flow deposits, composed by an older disrupted edifice (Mt. Somma) and an intra-caldera cone (Mt. Vesuvius) [34–44]. Volcanic activity in the area started 400 ka B.P. The Somma-Vesuvius volcanic succession mainly consists of lava flows, interbedded with strombolian scoria fall deposits (aged between 39 and 25 ka; Santacroce, 1987) overlain by the deposits of four main plinian eruptions—(i) Pomici di Base/Sarno (18 ka B.P.); (ii) Mercato/Ottaviano Pumice (8 ka B.P.); (iii) Avellino Pumice (3.5 ka B.P.); and (iv) Pompeii Pumice (79 CE).

Submarine canyons provide valuable information on the history of erosional and depositional processes on the continental slope [45–57]. They may represent sources of eroded sediments and/or pathways of sediment mass-transport, as well as sites of distinct depositional units [57–63]. The evolution of the canyon system is controlled by the interactions between gravity flow deposits and the seafloor morphology [64–66]. One of the most important processes responsible for the formation of the submarine canyons is represented by the channelization of sediment gravity flows into pathways of preferential erosion [54].

Tectonic activity and volcanism have been revealed to be important factors in controlling the morphology and evolution of submarine canyons, especially in geologically active continental margins [67–73]. The case history of the Dohrn and Magnaghi canyons represents a regional example of the important control of the tectonic setting coupled with volcanism on the morphology and the geologic history of submarine canyons. These controls have been documented for the Southern Ischia canyon system [74], whose eastern boundary has been controlled by a NE-SW normal fault, whereas the western boundary was influenced by volcanism, due to the growth of the Ischia Bank volcanic edifice.

The formation of the Dohrn canyon is genetically related with the main eruptive events involving the area offshore the Naples Bay, including the Campanian Ignimbrite (37 ky B.P.) [21] and the Neapolitan Yellow Tuff (15 ky B.P.) [75], which has been recently correlated with main tephra levels occurring in the northern Campi Flegrei offshore [76].

Many studies have been conducted on the origin of the Dohrn canyon in the last decades [77–82]. During the Late Quaternary, the continental slope of the Naples Bay was characterized by slumping and canyon formation. The Dohrn canyon has been interpreted as a submarine valley incised along a continental slope subject to a progressively decreasing slope gradient due to a fault block rotation [77]. A major erosional surface has been recognized toward the upper part of the Dohrn canyon slopes. This surface likely formed during the eustatic sea-level fall between 90 ka and 35 ka. It has been suggested, however, that the eustatic sea-level falls alone cannot account for the canyon's formation. Consequently, the formation of the Dohrn canyon has been interpreted as the result of the combined effect of eustatic sea-level fall and tectonic uplift, accompanied by relatively high sediment supply due to the vicinity of a river mouth on the shelf edge (Schiazzano river) [77].

Other studies have proposed that the Dohrn canyon represents a fossil drainage system of an active volcanic area [78]. The trend of its lower course is controlled by two main morpho-structural lineaments of the Naples Bay, such as the Banco di Fuori and Capri structural highs. Retreat of the canyon heads has been observed both in the Magnaghi canyon and in the western branch of the Dohrn canyon.

The upper section of the Dohrn canyon consists of two major curved branches, namely, a western branch (DWB) and an eastern branch (DEB). The DWB connects with the continental shelf through

the “Ammontatura” channel, representing an incised valley. The DEB has a meandering trend, starting from the shelf-break of the Sorrento Peninsula [78]. The upper section of the Dohrn canyon is characterized by V-shaped erosional profiles, whereas U-shaped profiles, mostly associated with depositional processes, prevail in the lower section of the canyon, suggesting recent phases of canyon filling. A number of terrace rims have been observed along the canyon flanks, suggesting at least three phases of incision and terracing of mature stage.

An area of the Dohrn canyon showing evidence of palaeo-landslides has been selected in order to evaluate the wave run-up generated by an estimated flow and using a recent theoretical model [79]. The main slide scars are located on the DWB head, where the canyons system is characterized by several terraces and by rectilinear gullies, likely due to tectonic control on the seafloor morphology of this area (western slope of the DWB) that connects the Banco di Fuori morpho-structural high with the continental slope north of the Capri structural high [79]. Numerical modeling has been constrained through a bathymetric profile, which shows a detachment area about 475 m wide, located at water depths of 380–450 m.

A unique and threatened deep-water coral-bivalve biotope, new to the Mediterranean Sea offshore of the Naples megalopolis, has been recently detected in the Dohrn canyon, based on ROV transects [82]. If compared with the cold-water habitats of the Mediterranean Sea, the Dohrn canyon reveal a particular oceanographic and ecological interest, also indicated by the co-existence of living bivalves with the cold-water corals. The data shown in this study also suggest that hot spots of deep-sea benthic biodiversity may coexist with anthropogenic impacts, such as litter, plastic material and long lines [82].

In this work, we present an integrated stratigraphic study of geophysical and geological data acquired in the area of the Dohrn Canyon along the continental slope of the Naples Bay. Our results may contribute toward a better understanding of the sedimentary processes involved in the evolution of a canyon system that develops on a continental margin characterized by active tectonics and volcanism. The data discussed in this research also represent a relevant information for the evaluation and mitigation of natural hazards (i.e., volcanism, seafloor stability) within the context of management and planning of densely populated coastal areas.

2. Material and Methods

The acquisition of geological and geophysical data presented in this study has been carried out within the frame of a national project (CARG) for the geological mapping of Italy at 1:50,000 scale. The morphobathymetry of the Naples Bay has been obtained as a mosaic of Multibeam Echosounder (MBES) surveys conducted by the Institute of Marine Sciences of National Research Council of Naples, Italy, mostly between 2000 and 2014, using various MBES systems. The processing of multibeam data was carried out with PDS2000 software (Teledyne Marine, Cypress, TX, USA) following the International Hydrographic Organization standards [83]. Processing included the removal of navigation errors, noise reduction (i.e., despiking), removal of poor-quality beams, and tidal and sound velocity corrections. The final digital terrain model (DTM) derived from the MBES data covers an area of ~900 km² with a cell size of 10 m. Onshore topographic data were obtained from the official topographic grid of the Military Institute for Geography (20 m grid cell), acquired between 1985 and 1990 by aerial photogrammetry [84] (Figure 1).

The geological framework of the shallow structures has been investigated through seismic and sequence stratigraphic interpretation of a grid of multichannel and single-channel, high resolution (Sparker 1 kJ and 4 kJ) reflection seismic profiles. Selected sub-bottom Chirp profiles were also used to document the detailed stratigraphic architecture of channel-levee complexes and gravity flow deposits.

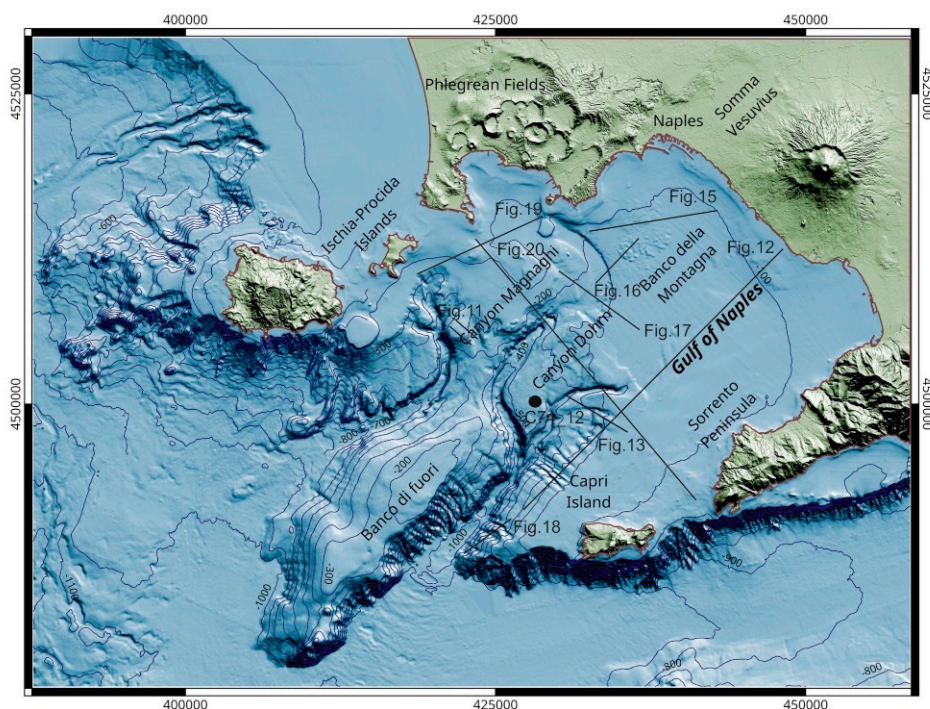


Figure 1. Digital elevation model (DEM) of the Naples Bay with location of seismic profiles and gravity core C74_12 discussed in this study.

The analysis of seismic reflection profiles was conducted according with the methods and procedures of seismic and sequence stratigraphic interpretation [85–91]. Seismic facies of stratigraphic units identified on seismic profiles were described particularly based on the internal and external geometries of individual units and on the continuity, amplitude, and frequency of reflectors [92–96]. Relative sea-level fluctuations were analyzed by constructing chronostratigraphic diagrams and curves of relative sea-level cycles [90,91].

The interpretation of reflection seismic data was calibrated with integrated stratigraphic analysis of gravity core C74_12, collected at a water depth of 586.6 m, along the Dohrn canyon (Figure 1). Core samples were half-split, photographed, and described at cm-scale using a 10× lens. Microscope observation was conducted on selected samples of sieved sand fraction to identify the major lithologic components (lithoclasts, bioclasts, volcanoclasts) and determine the shape and surface texture of particles. Sedimentological analysis included the recognition of major lithofacies associations, sedimentary structures, and grain-size analysis of the fraction <63 μ by laser diffractometry (Sympatec). A total number of 81 samples have been processed for the grain-size analysis. Statistical parameters have been calculated according to the classic graphical equations of Folk and Ward (1957) [97].

The analysis of sediment samples has been complemented by high-resolution (2 cm step) measurements of physical properties of core C74_12 to assist stratigraphic correlation. Core logging was conducted on half-split cores, using a fully automated multi sensor core logger (MSCL-Geotek) (Geotek, Northamptonshire, UK) at the CNR-ISMAR petrophysical laboratory. The MSCL system includes (i) a Bartington MS2E Point sensor, to measure the low-field volume magnetic susceptibility; (ii) a gamma ray attenuation porosity evaluator (GRAPE) sensor to determine the bulk density; (iii) an ultrasonic P-wave (PWTs) system to analyze the P-wave velocity through the core; and (iv) a Minolta Spectrophotometer CM 2002 to detect the reflectance (L%), acquired within 1 h after the core splitting to minimize redox-associated color changes.

3. Geological Setting

The Gulf of Naples stretches in the southern part of a tectonic depression, namely the Campania Plain, whose formation was controlled by the Neogene back-arc extension of the Tyrrhenian Basin that accompanied the northeastward-verging accretion of the Southern Apennines during the roll-back of the subducting Adriatic plate [98–105]. The Early Pleistocene marks the onset of NW–SE extension and tectonic subsidence of the Campania Plain–Napoli Bay basin, whereas a following phase (Middle Pleistocene in age) mainly resulted in NE–SW extension. Normal faults associated with these two phases were later reactivated during the Late Pleistocene–Holocene and caused either subsidence or tectonic uplift, especially in areas affected by volcano-tectonic deformation [106–112].

The regional geological structure of the Naples Bay is characterized by prevailing NE–SW and ENE–WSW trends of normal faults, namely expressed in the directions of the Dohrn canyon and the Capri-Sorrento lineament (Figure 2) [113]. These faults have often accommodated significant offsets within the Meso-Cenozoic sedimentary succession, representing the acoustic basement on the seismic profiles in the area.

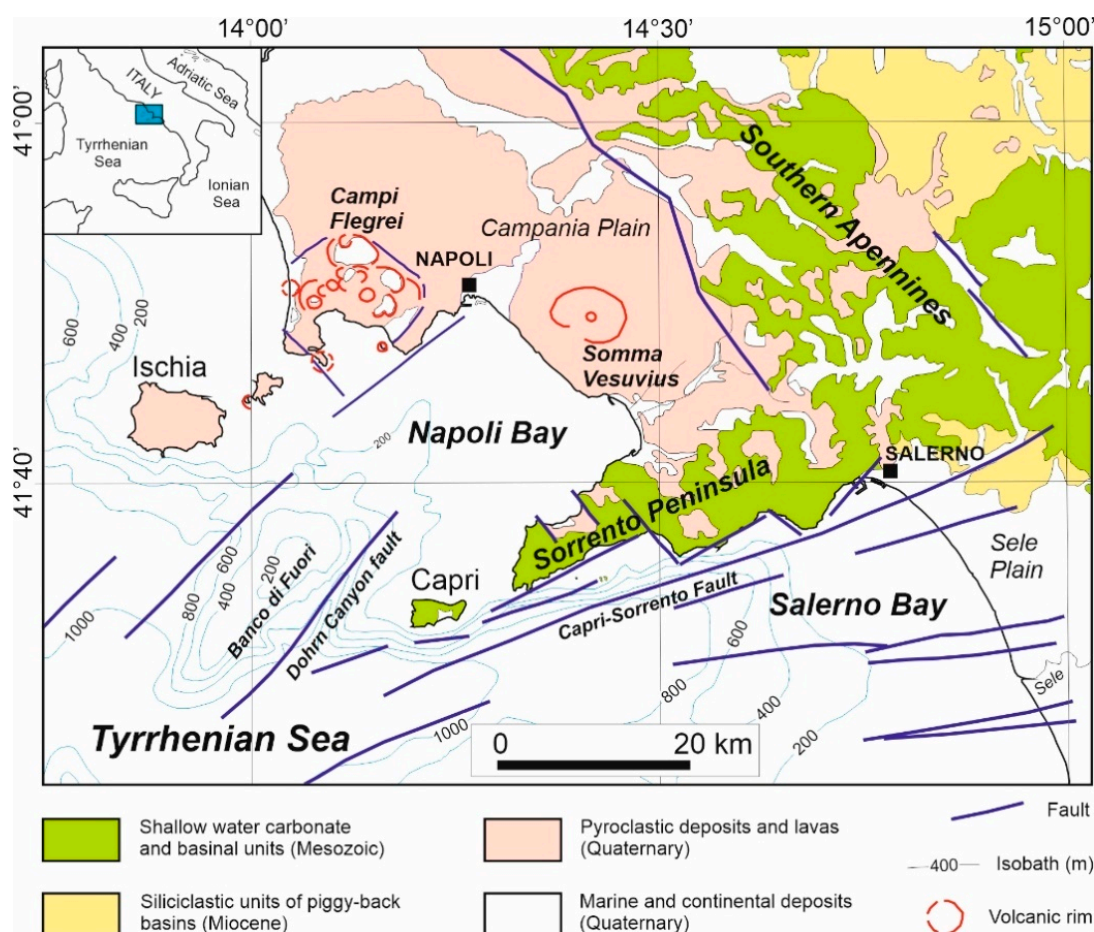


Figure 2. Geological sketch-map of the Naples Bay. The location of the Dohrn canyon fault and Capri-Sorrento fault has also been reported.

The present-day morpho-structural setting of the Campania continental margin and the Naples Bay is the result of significant interaction between volcanic and sedimentary processes during the Late Quaternary [114]. The Dohrn canyon fault bounds the south-western flank of the Banco di Fuori, with a total offset between the top of the structural high NW of the fault and the top of the downthrown Meso-Cenozoic carbonates below the Dohrn canyon, SE of the fault, in the order of one thousand meters. The enhanced thickness of the Middle-Late Pleistocene prograding wedge associated with the

Dohrn canyon fault suggests a coeval age for tectonic activity along this structure, which is then buried by relatively undeformed Holocene deposits.

Based on previous seismic data, three regional geological sections have been constructed across the Campania continental margin (Figure 3) [113], showing the main morpho-structures occurring at a regional scale (“Banco di Fuori” morpho-structural high, Dohrn canyon, Magnaghi canyon, Capri Basin, Salerno Valley, Volturmo basin).

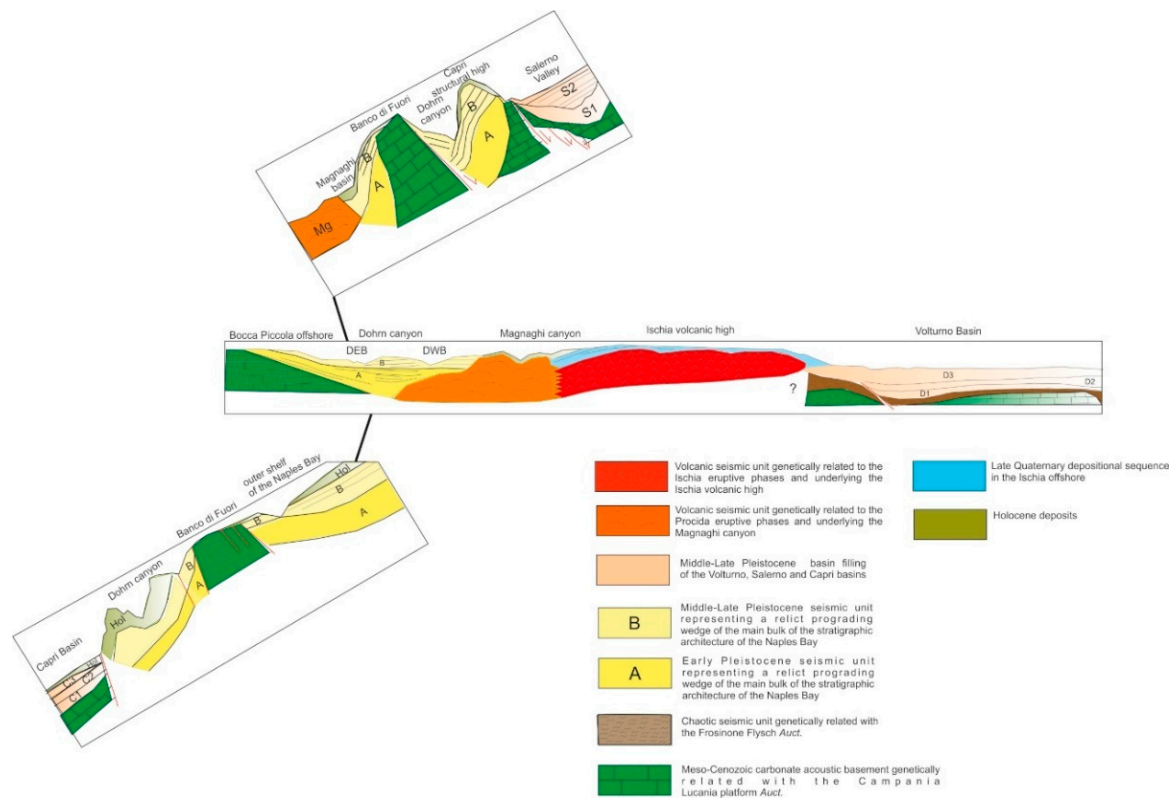


Figure 3. Geological sketch-sections on the Campania continental margin after Aiello et al., 2011 [113], showing the main morpho-structures on a regional scale (Banco di Fuori morpho-structural high, Dohrn canyon, Magnaghi canyon, Capri Basin, Salerno Valley, Volturmo Basin).

“Banco di Fuori” is a morpho-structural high composed of Meso-Cenozoic carbonates bounding the Naples Bay to the south. The flanks and top of this high are overlain by a thick succession of Pleistocene deposits. The Dohrn canyon is a major erosional lineament that broadly divides the Naples Bay into an eastern sector, mostly characterized by siliciclastic deposits, and a western sector where volcanic and mixed volcanoclastic-siliciclastic units prevail. The canyon is composed of two branches, which converge into a NE–SW thalweg, bounded by the Capri Basin to the South. The Magnaghi canyon, located to the West of the Dohrn canyon, is characterized by diffused erosional processes along its flanks accompanied by the occurrence of volcanoclastic gravity flow deposits along the main axis of the valley, mostly fed by the products of the eruptive activity of the Ischia and Procida islands during the Late Quaternary. The Capri Basin forms a deep basin located in the Tyrrhenian bathyal plain south of the Naples Bay and filled by a several hundred meters of Pleistocene–Holocene sediments overlying the Meso-Cenozoic carbonate acoustic basement. The Salerno Valley is a half-graben basin characterized by three seismic units composed of Quaternary marine and continental deposits, laterally resting above chaotic deposits of the Cilento Group. Off the northern sector of the Campania Plain, the Volturmo Basin is filled up by a thick succession of Quaternary marine siliciclastic, volcanoclastic and deltaic units, overlying a substrate of Meso-Cenozoic carbonates and Miocene deposits (sand and shale).

Campi Flegrei is volcanic district along the coastline of the Naples Bay, where volcanism has been active since ~60 ka B.P. [18,21–24,32,33,115–122]. The area was characterized by a large caldera forming eruption, which caused the emplacement the Campanian Ignimbrite, (ca. 39 ka B.P.). The regressive peak of the last glacial maximum (isotopic stage 2) resulted in ca. 30 km progradation of the shoreline that reached the present-day location of the shelf break in the Gulf of Naples, close to the 140 m isobath. The glacio-eustatic emersion was accompanied by significant volcanoclastic input and aggradation of the Campania Plain, following the deposition of the Campanian Ignimbrite [18–22,24,32,33,117,123–125]. Later on, another ignimbritic eruption of Campi Flegrei led to the formation of Neapolitan Yellow Tuff (NYT) [123].

Previous interpretations have suggested that the Campanian Ignimbrite possibly originated along a NW–SE trending normal fault (Napoli-Vico Equense normal fault) [124] that caused the tilting of coastal plain toward the NE. The tilting block was bounded by NE–SW trending normal faults, located along the northern coast of the Sorrento Peninsula and along the opposite side of the Gulf of Naples. A significant lineament pertaining to this structural trend is represented by the Acerra-Dohrn canyon fault, which extends onshore from the Acerra graben to the Dohrn canyon offshore [124–127]. During the last decades a series of detailed studies on the Campania Ignimbrite deposits and the crustal mechanisms controlling the emplacement of the ignimbrites of the Campania Volcanic Zone (CVZ) have been presented [32,123–125,128–131].

Absolute age determinations on the products of the CI yielded ca. 37 ka BP [131,132], 39 ky [130], and 39.85 ± 0.14 ka B.P. [133], whereas the NYT has been dated to ca. 15 ka B.P. [75]. In the northern CVZ, the stratigraphic data from more than 600 boreholes [19,134,135] allowed the construction of geological sections showing the stratigraphic architecture of the ignimbrite deposits [123] (Figure 4). Figure 4 shows that the lowermost unit is composed of marine sediments (Tyrrhenian Layer M1), whose top has been dated at 126 ka B.P. [134]. A volcanic unit overlies the marine deposits and is composed of massive ignimbrite deposits and lava flows. This unit is overlain by another succession of marine deposits, dated at 55–50 ka (Tyrrhenian unit M2) [134], which is covered in turn by the CI deposits. The Giugliano Ignimbrite (GI) follows above the CI deposits. The intermediate CVZ, whose stratigraphy is described in Figure 4 [123], is characterized by the occurrence of the NYT caldera, in its western sector, whereas its eastern sector occupies the area close to the town of Naples.

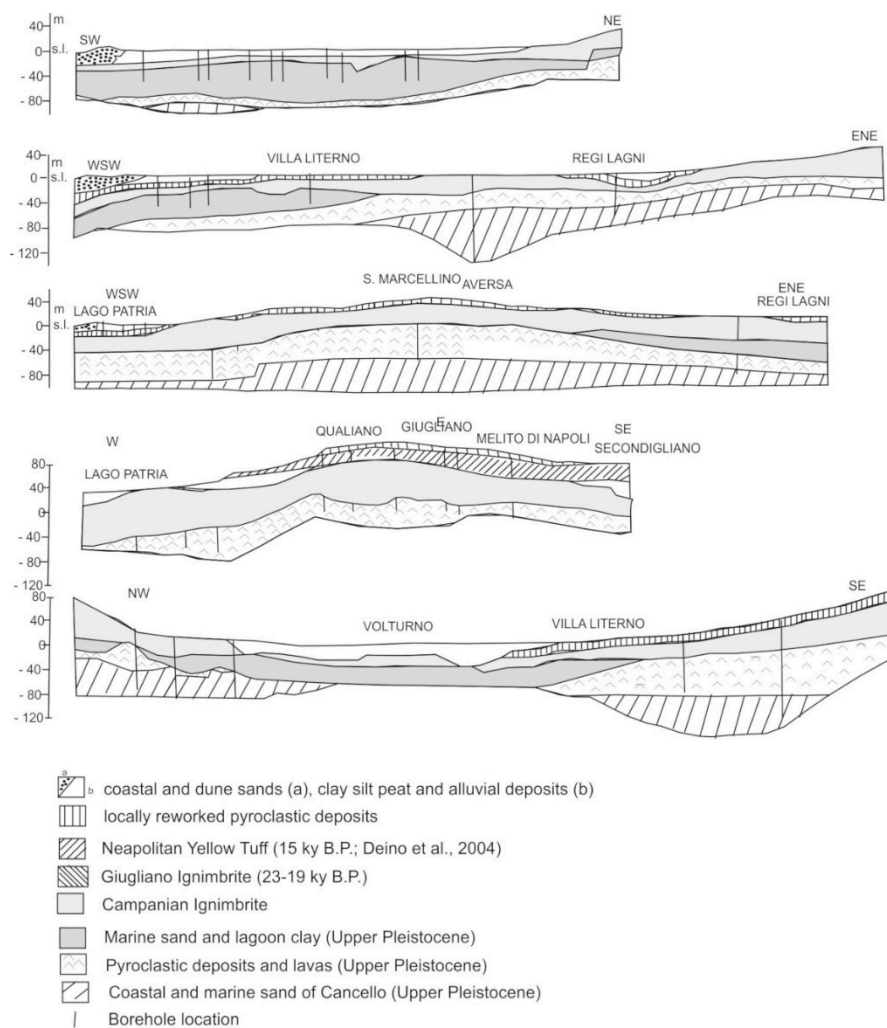


Figure 4. Geological sections and location of boreholes in the Northern CVZ, modified after Rolandi et al., 2003 [123].

4. Results

4.1. Morpho-Bathymetry and Gravity Instabilities of the Naples Bay Canyons

An extensive, high-resolution bathymetric survey of the continental shelf/slope system of the Campania region (southern Italy) has been carried out in the frame of research programs of marine geological mapping. The relative bathymetric data were acquired between 1997 and 2017, using multibeam systems with an average vertical resolution of $<0.25\%$ water depth and a position accuracy of <10 m. The survey data were successively merged with a Digital Terrain Model (DTM) created from topographic maps of the Naples Bay onshore coastal area and islands, to produce a Digital Elevation Model (DEM) based on a homogeneous grid with cell-spacing of 20 m (Figure 5) [78]. Major morphological elements of the Naples Bay include: (1) the Dohrn-Magnaghi canyon system, carving the continental slope at water depths between -250 m and -1100 m [77–80,136–139]; (2) the continental slope system of the Ischia island and related submarine canyons [74]; (3) the onshore and offshore volcanoes of the Campi Flegrei (Pentapalumbo, Nisida, and Miseno banks) [18,21,28,30–33]; (4) the rough sea bottom area of the outer shelf of the city of Naples (Banco della Montagna) [78,81,137–139]; (5) the sediment wave field of the inner continental shelf off the Vesuvius [34,35,78,81,137–140].

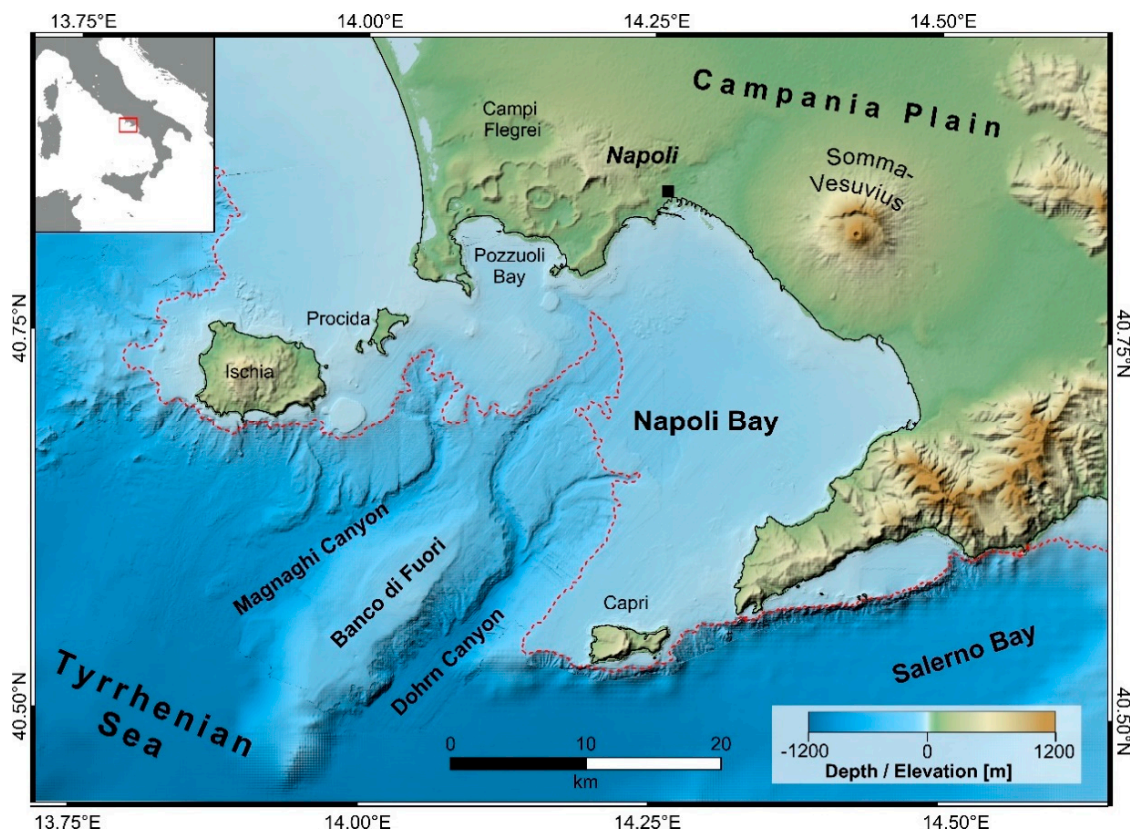


Figure 5. Morphologic setting of the Naples Bay; dashed line indicates the 200 m isobaths, which approximately individuates the shelf break; modified from Sacchi et al., 2019 [141].

The Dohrn canyon represents the most important morphological feature of the Naples Bay and develops into two branches that converge into a main valley. The thalweg of the canyon is relatively flat and displays a variable width (200 m–1 km). The canyon slopes are relatively steep, sometimes terraced, and are characterized by several instability phenomena, such as slide scars, slumps, and slides. On the southeastern flanks of the canyon system, at least four rectilinear, sub-parallel incisions occur, likely because of a structural control by ENE-WSW trending faults (Figure 5).

The Naples canyon system originates from the shelf break off the Campi Flegrei volcanic district along the 140 m isobath. The general morphological setting of the canyon system is controlled by two major morpho-structural lineaments of the Naples offshore, namely the Banco di Fuori structural high, bounding the canyon system to the South and the Capri structural high, bounding the Dohrn canyon to the East, next to its confluence with the bathyal plain. Both the Magnaghi canyon and the western branch of the Dohrn canyon show morphological evidence of retreatment of the canyon heads. Particularly, the Dohrn shows two retrogressive head areas, as documented by the multibeam bathymetry and morpho-bathymetric profiles.

4.1.1. Geomorphologic Map of Naples Canyons

Based on marine DTM derived by MBES data, a geomorphologic interpretation of the Dohrn canyon and of the continental slope of the Naples bay was obtained. Major morphological lineaments of the canyon system include the main drainage axes, slide scars, and associated gravity instability areas, relict volcanic edifices, shelf break, terraces, and gravity flow deposits (e.g., turbidite slope fans; Figure 6). The Dohrn canyon is fed by several tributary channels, which can be readily identified from morpho-bathymetric interpretation. Two main tributary channels originate from the shelf break of the Naples Bay, located approximately along the 140 m isobath and cross the entire continental slope between the Dohrn and Magnaghi canyons. A system of tributary channels, developing at water

depths between 200 m and 500 m, feeds the Dohrn eastern branch from the shelf break of the Sorrento Peninsula. A remarkable rectilinear shape of the channels in plain view suggests a structural control on the morphology of the drainage system.

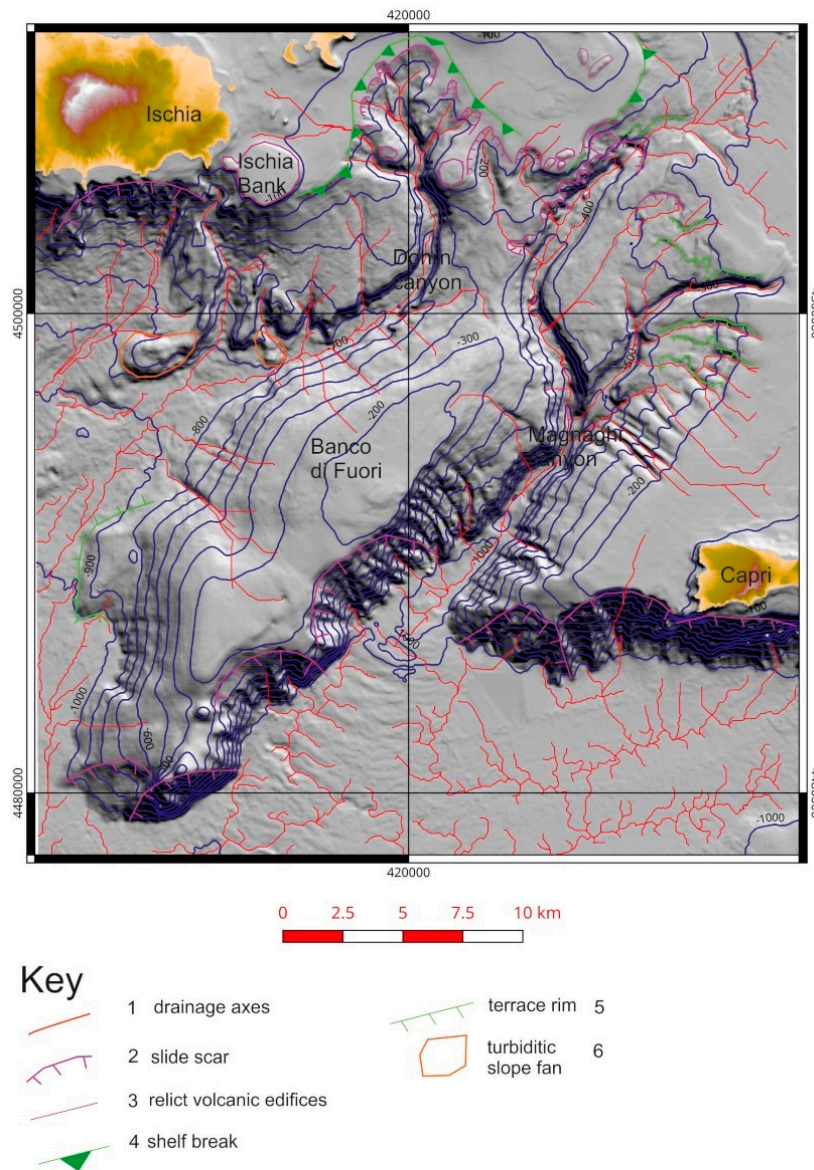


Figure 6. Geomorphologic map of the Naples canyons.

4.1.2. Bathymetric Profiles

Two bathymetric profiles perpendicular to the main axis of the Dohrn canyon have been constructed (Figures 7 and 8). At the canyon head, the Dohrn drainage system is characterized by two main tributary channels. The western tributary is deeper and more incised than the eastern one (P1; Figure 8). Profile-P2 represents the sector of the canyon system where the two tributary channels merge to form a single valley involved by severe erosional processes, particularly to the NW and W of the Capri Basin [139].

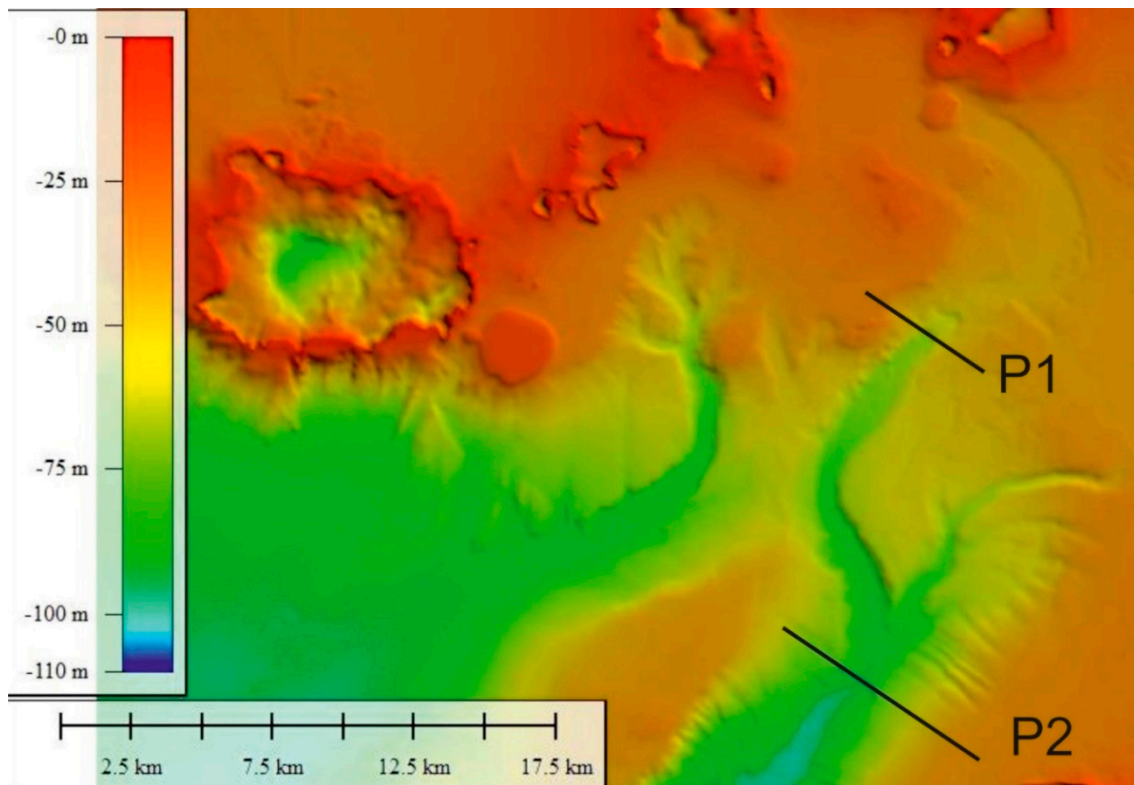


Figure 7. Digital terrain model (DTM) with location of the trace of the bathymetric profiles analyzed in the Dohrn canyon.

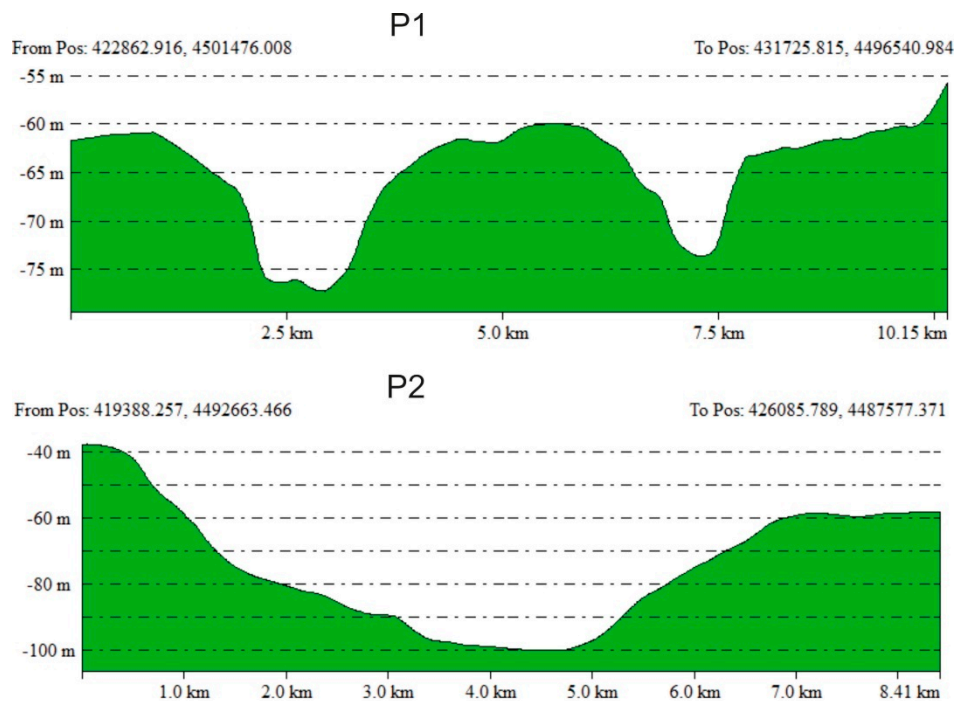


Figure 8. Bathymetric profiles crossing the Dohrn canyon (see Figure 7 for the location).

The central-eastern part of the Naples Bay is characterized by the occurrence of the Ammontatura channel, a relatively minor incision of the Dohrn canyon system characterized by a curved morphology in plain view, a flat thalweg and asymmetrical (locally irregular) slopes. Ammontatura channel originates from a narrow area between the Nisida island and the Nisida bank and terminates at the

head of the western tributary channel of the Dohrn canyon (Figures 9 and 10). It also separates the “Banco della Montagna” structure from the volcanic margins of the Campi Flegrei Bathymetric profiles indicate that the western slope of the Ammontatura Channel is generally steeper than the western slope, where evidence of a series of terraced surfaces is also documented. The valley is 2.5 km wide and ca 20–40 m deep. In its northernmost part, the axis of the channel bends toward the north-west and terminates abruptly N of the Nisida Bank.

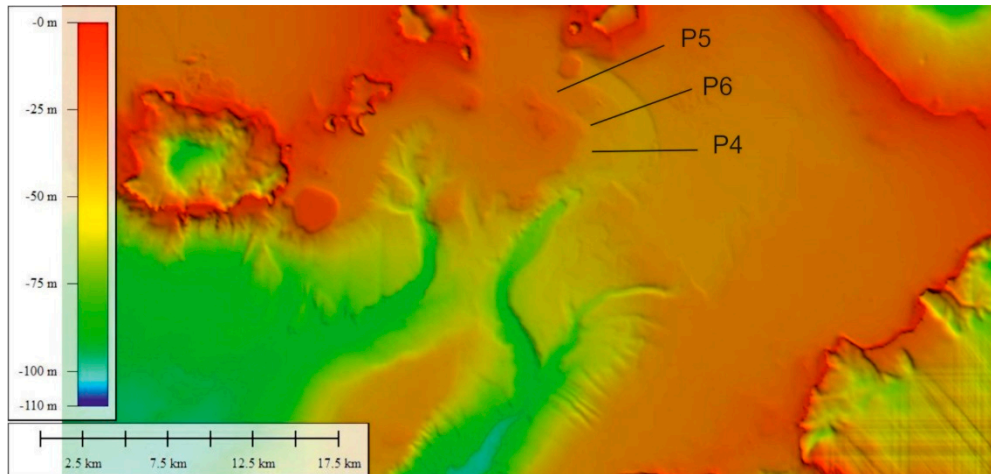


Figure 9. DTM with location of the trace of the bathymetric profiles analyzed in the Ammontatura channel.

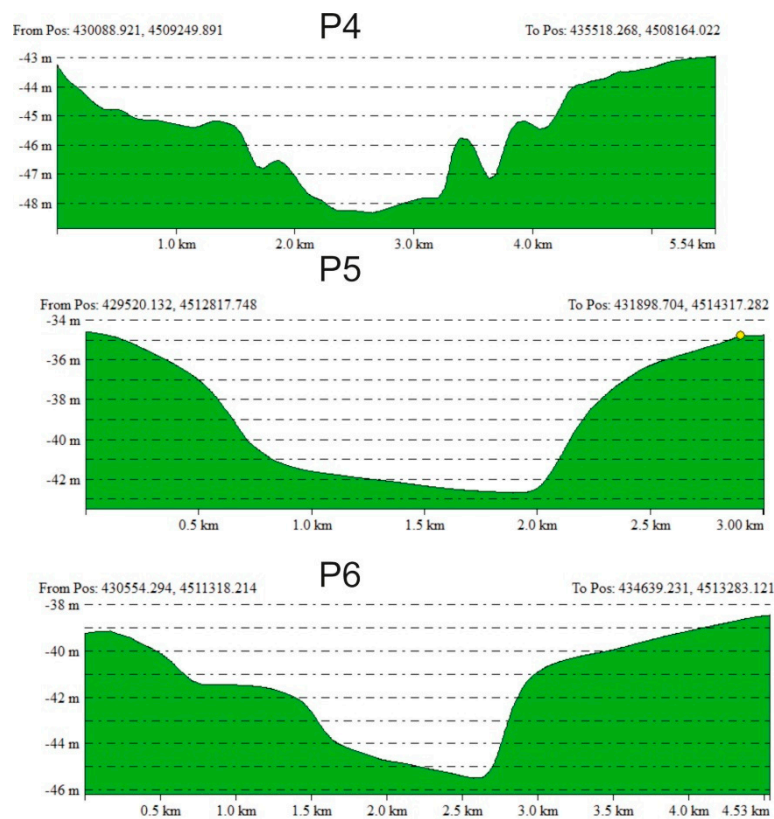


Figure 10. Bathymetric profiles of the Ammontatura channel.

4.2. Main Seismic Facies Recognized on Subbottom Chirp Profiles

4.2.1. Channel-Levee Complex

Seismic facies interpreted as channel-levee complexes have been identified on subbottom Chirp profiles crossing the Ammontatura channel (Figure 11). This facies is characterized by alternating sub-parallel seismic reflectors and acoustically transparent intervals, separating an incision, lacking filling, and corresponding with the channel. This facies is composed of gravity flow (e.g., turbidite, debris flow) deposits, characterized by alternating sands and muds, that can be interpreted as channel-levee complexes in the areas surrounding the Dohrn canyon and the related tributary channels.

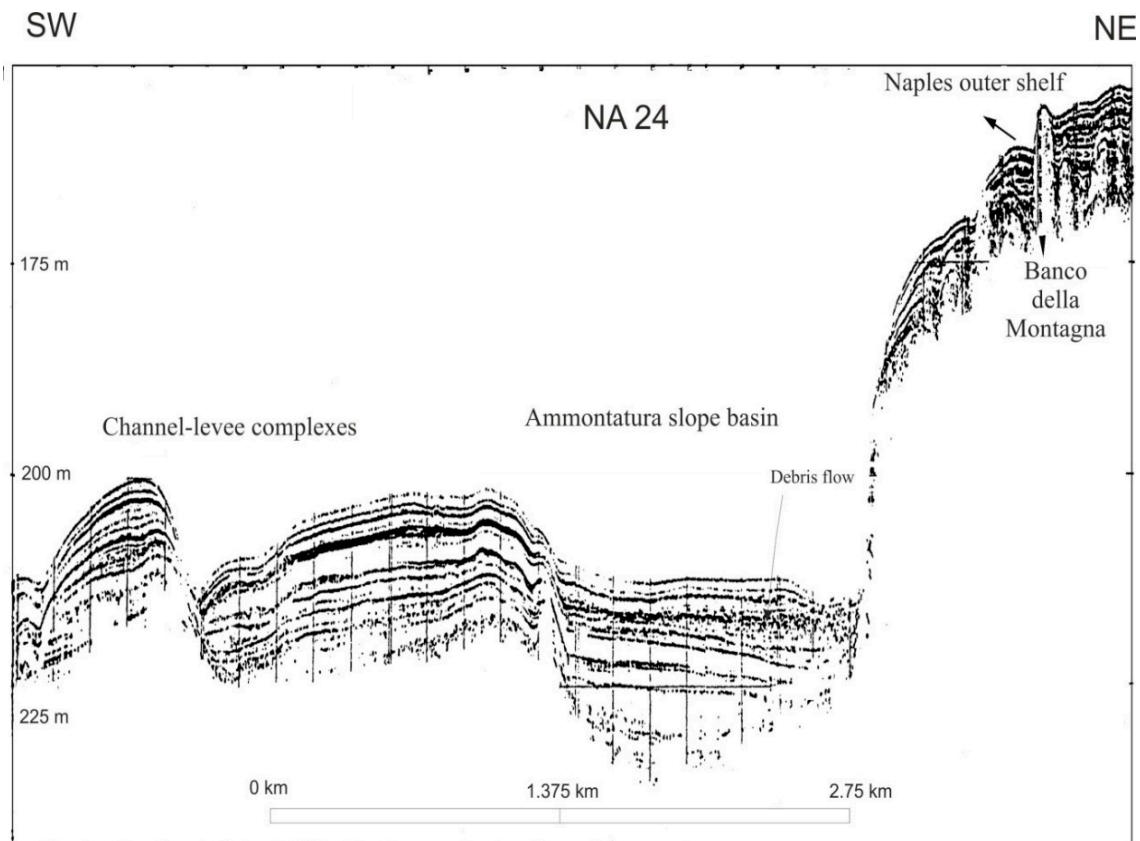


Figure 11. Subbottom Chirp profile NA24, showing significant seismic facies occurring in the Naples Bay.

Channel-levee complexes have been also documented by Chirp profiles NA18 (Figure 12) and GP23 (Figure 13). Profile NA18 shows the continental shelf of the Naples Bay, the Ammontatura channel, a slope morphological high and the Pentapalummo Bank, with its SE slope cut by a tributary channel (Figure 12). The Naples continental shelf is characterized by wavy, sub-parallel and continuous seismic reflectors, whereas the Ammontatura channel shows a sequence of chaotic seismic reflectors, overlain by parallel seismic reflectors. The slope morphological high is characterized by wavy and sub-parallel continuous seismic reflectors and the Pentapalummo bank shows an acoustically transparent seismic facies (Figure 12). Sub-parallel and continuous seismic reflectors on the continental shelf of the Naples Bay have been interpreted as Holocene marine deposits, whereas the chaotic sequence recognized in the Ammontatura channel has been interpreted as corresponding to slump deposits, overlain by sub-parallel Holocene marine strata (Figure 12). Wavy and sub-parallel reflectors forming most of the slope morphological high have been interpreted as channel-levee complexes, whereas the acoustically transparent seismic facies on the Pentapalummo bank have been regarded as representing the volcanic acoustic basement (Figure 12).

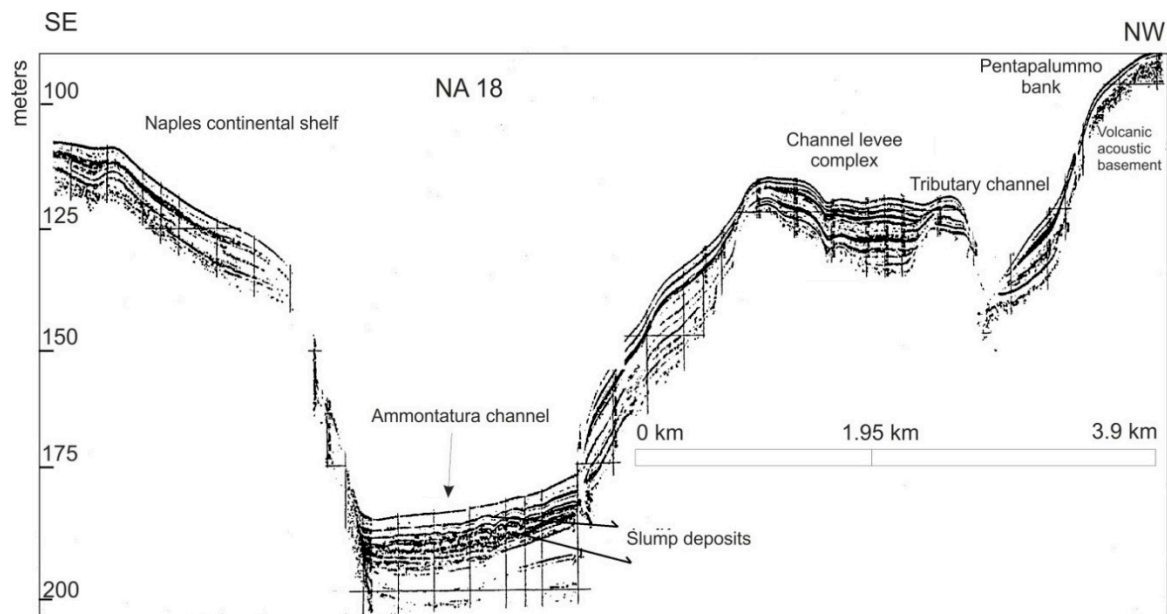


Figure 12. Subbottom Chirp profile NA18, showing channel levee complexes occurring in Naples Bay.

Seismic profile GP23 crosses a relict morphology of the Late Pleistocene continental shelf, located in the central slope of the Naples Bay and the continental slope towards the thalweg of the Dohrn eastern branch (Figure 13). The relict morphological high is characterized by seismic facies showing prograding clinoforms systems, truncated at the top by an angular unconformity and overlain by parallel seismic reflectors (Figure 13). The continental slope shows inclined seismic reflectors and significant detachment scours (Figure 13), whereas at the base-of-the-slope truncated reflectors and thin sediment drapes draping on the canyon walls are also documented (Figure 13; refer to the B rectangle on the figure). The prograding clinoforms detected on the relict morphological high have been interpreted as Middle-Late Pleistocene continental shelf deposits, truncated by an erosional unconformity and overlain by Holocene marine layers (Figure 13). Thin Holocene marine deposits also drape older strata truncated along the channel walls (Figure 13).

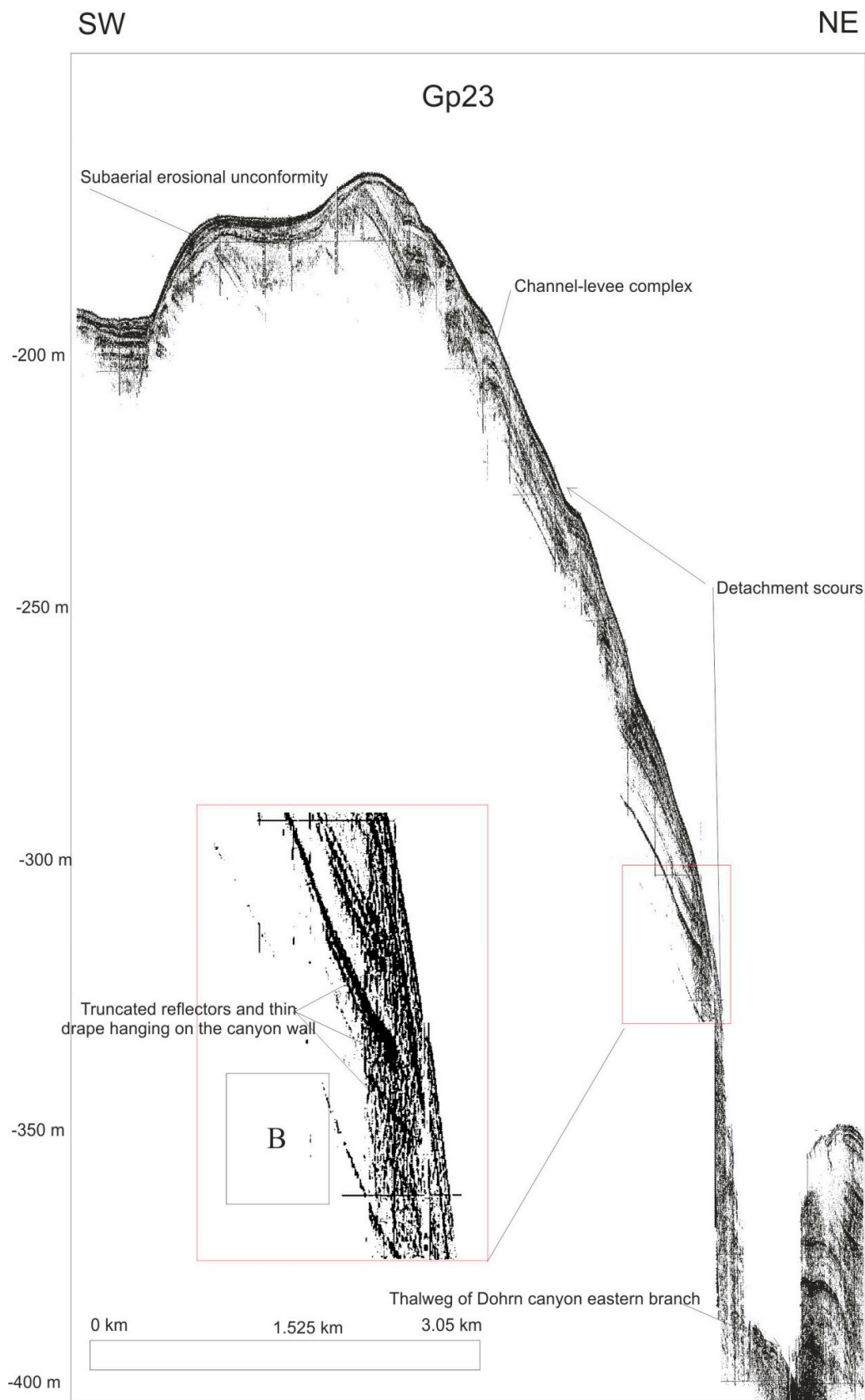


Figure 13. Sub-bottom Chirp profile GPNA23, showing channel levee complexes occurring in the Naples Bay and canyon morphology.

4.2.2. Gravity Flow Deposits

Seismic units represented by lenticular bodies with chaotic reflections, poor lateral continuity of seismic reflectors and a turbid acoustic facies (Figure 11) are often found sandwiched between acoustically sharp, wavy inclined reflectors, and have been interpreted as corresponding to gravity flow (e.g., debris flow/turbidite) deposits formed along the continental slope.

A sketch table was constructed in order to summarize the most significant seismic facies detected in the Naples Bay on sub-bottom Chirp profiles and their corresponding seismic stratigraphic interpretation (Figure 14). It should be noted that the table is based on previously published data [142] and includes a wider spectrum of seismic facies than that specifically discussed in this work. Chaotic reflectors with poor lateral continuity and transparent to turbid facies have been interpreted as volcanoclastic and/or pyroclastic deposits (mud flows, lahars, pyroclastic flows) and are genetically related to the Somma-Vesuvius volcano (A in Figure 14). Convex and acoustically transparent units, partly exposed at the sea floor, alternating with wavy or parallel reflectors with a clear acoustic appearance have been interpreted as volcanoclastic mounds composed of alternating coarse-grained pumice, volcanic sand and mud (B in Figure 14). These features occur as a field of small mounds (Banco della Montagna) that develop over the continental shelf of the Naples Bay and have been recently interpreted as the result of dragging and uplift of unconsolidated volcanoclastic deposits from deeper stratigraphic layers due to the degassing of overpressured volcanic fluids originated from deeper structural levels [81]. Convex units with fair lateral continuity of with a transparent acoustic facies, resting above high amplitude reflectors have been recently interpreted as Holocene marine sediments involved by gravitational instability and slow creep over a basal sliding surface likely corresponding to a maximum flooding surface (MFS) (C in Figure 14). Slightly inclined acoustically clear, parallel reflections, passing upwards to an area with a turbid acoustic appearance have been interpreted as outcrops of relict sands, deposited during the last sea level lowstand (18–20 ky B.P.), which is genetically related to the last 4th order eustatic cycle (D in Figure 14). Acoustically transparent bodies (E in Figure 14), respectively, correspond to the dome-shaped volcanic units genetically related to (i) Campanian Ignimbrite (E1 in Figure 14); (ii) volcanic acoustic basement detected at Pentapalumbo, Miseno, and Nisida banks (E2 in Figure 14); and (iii) volcanic basement interpreted as lava flows of parasitic vents genetically related to the Somma-Vesuvius volcano (E3 in Figure 14). Gravity flow (debris flows/turbidite) deposits have been documented as lenticular bodies with chaotic laterally discontinuous reflectors with a turbid acoustic appearance (F in Figure 14). Channel-levee complexes have been characterized as a succession of convex and sub-parallel or inclined reflectors with good lateral continuity, with channel and embankment morphologies (G in Figure 14). A succession of inclined and wavy reflectors with a good lateral continuity and sharp to turbid acoustic characters have been interpreted as a relict morphology of the Middle-Late Pleistocene continental shelf, which is genetically related to the Sarno prograding wedge (H in Figure 14).

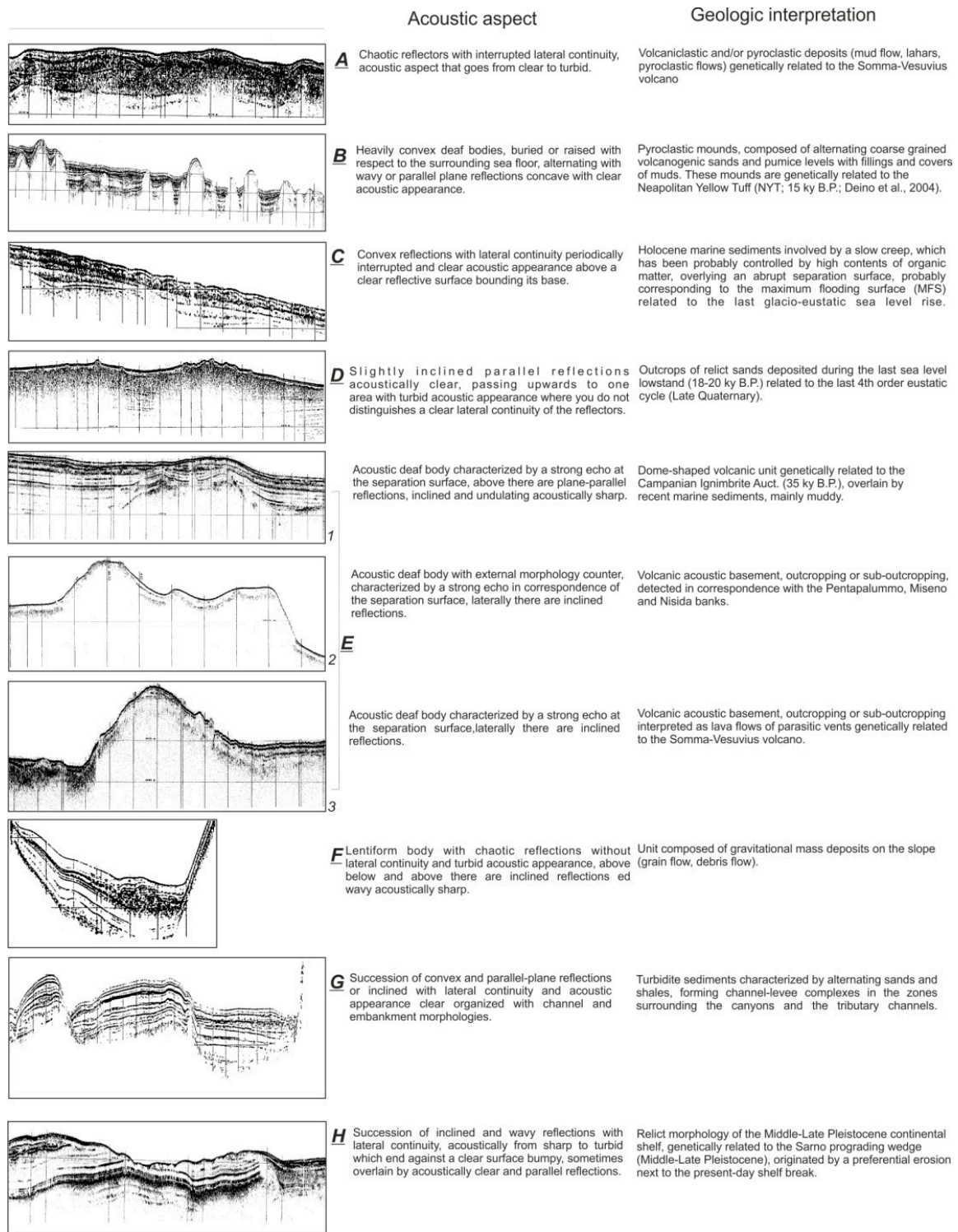


Figure 14. Sketch diagram of selected Subbottom Chirp profiles recorded in the Naples Bay, highlighting the acoustic aspect and the corresponding geologic interpretation (modified from Aiello et al., 2009 [142]).

4.3. Seismic Stratigraphy

Erosion and the transport of sediments in the Bay of Naples are chiefly driven by the Dohrn and Magnaghi canyons, which expose along its walls hundreds of meters of a Middle-Late Pleistocene prograding wedge represented by siliclastic and volcaniclastic deposits, genetically related to the paleo-Sarno fluvial system. The Dohrn canyon is separated from the Magnaghi canyon by a major

morpho-structural high (“Banco di Bocca Grande” or “Banco di Fuori”), likely formed as a result of the local uplift and tilting of the basement rocks (Mesozoic carbonates) that are widely exposed in the Sorrento Peninsula—Capri Island structural high.

The location of the DEB (Dohrn eastern branch) and several lines of evidence deriving from seismic stratigraphic interpretation have suggested a genetic linkage between the activity of the Dohrn canyon and the Sarno paleo-drainage system during sea-level lowstands. A 30–40-m-thick seismic sequence overlying older, undisturbed reflectors and including channel-levee complexes, crops out at the sea floor on both the sides of the DEB. These deposits do not seem related to the main branches, which are deeply incised, but rather than the occurrence of tributary channels, controlling the overflow of sediment fluxes in the surrounding areas.

The deltaic system of the paleo-Sarno river has directly fed the continental slope areas during the lowstand phases of the Middle-Late Pleistocene, producing a large and thick prograding wedge, deeply incised by the Dohrn canyon (Figure 15). We infer that the DEB was directly linked with the paleo-Sarno river mouth during lowstand phases. This is also suggested by the occurrence of two non-volcanic morphobathymetric highs detected on Chirp profiles close to the heads of the Dohrn canyon, (Figure 13). Seismic-stratigraphic analysis shows they represent deltaic sediments arranged with clinoform patterns and suggest they are related to the distal part of the prograding wedge fed by the paleo-Sarno river mouth. These features reach an elevation of 20–30 m with respect to the surrounding seafloor water depth and may be interpreted as relict morphologies of the Middle-Late Pleistocene continental shelf (Figure 16). The origin of these morpho-bathymetric high was likely the result of differential erosion during the subaerial exposure of the continental shelf following sea level lowstand. Seismic interpretation also suggests this erosional phase predates the eruption of the Campanian Ignimbrite age (39 ka B.P.).

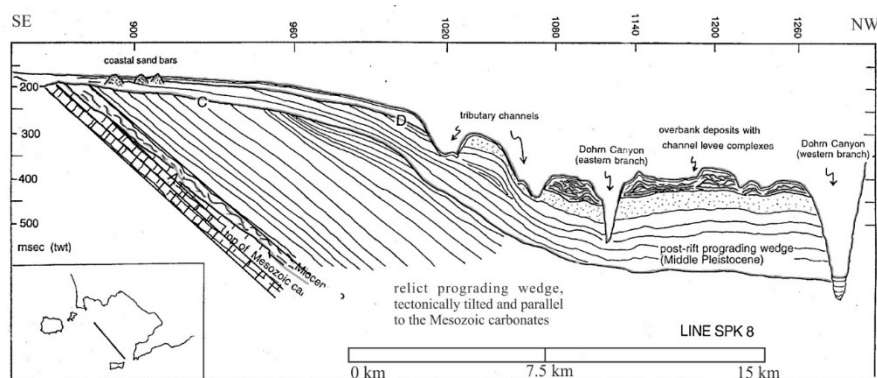


Figure 15. Geologic interpretation of the Sparker seismic profile SPK8. Note that the Mesozoic carbonate acoustic basement of the Naples Bay is overlain by several stratigraphic sequences, including the pre and syn-rift prograding wedge, Early-Middle Pleistocene in age and the post-rift prograding wedge, Middle Pleistocene in age. C and D represent main regional unconformities.

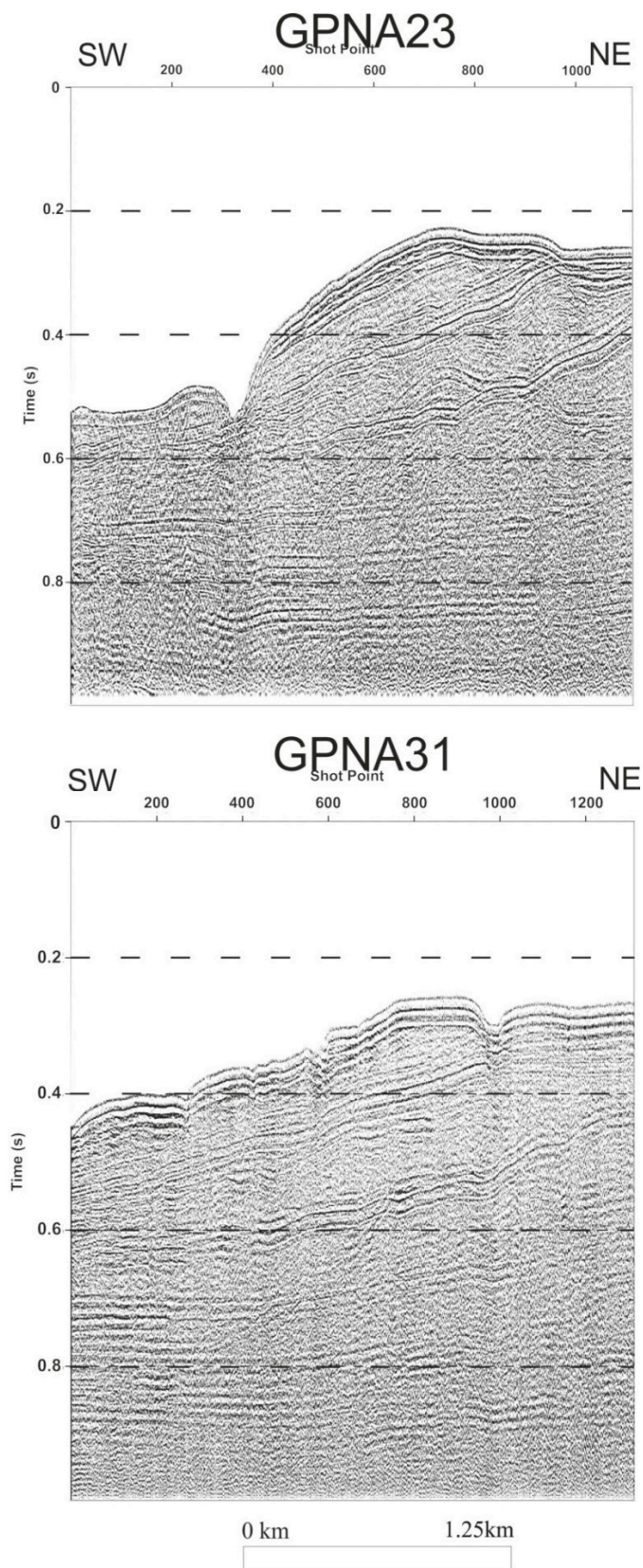


Figure 16. Details of the multichannel Watergun seismic lines GPNA23 and GPNA31 crossing the relict morphologies of the Middle-Late Pleistocene continental shelf located at the center of the Naples Bay.

Selected single-channel (Sparker) profiles have been interpreted in order to illustrate the main seismic-stratigraphic units recognized in the Naples Bay (SP20, SP20_1, SP2, SP3; Figures 17–20). Seismic line SP20 documents the stratigraphic setting of the continental shelf area of the Naples Bay, that is characterized by three main seismic units (Figure 17). The lowest unit is represented by truncated prograding clinoforms and has been interpreted as a relict prograding wedge fed by the Sarno river mouth, probably Middle-Late Pleistocene in age. This succession is overlain by a thick acoustically transparent seismic unit, likely corresponding with the Campanian Ignimbrite, [15–27,29], whose submarine occurrence in the Naples Bay has been recently mapped by Aiello et al., 2016 [31]. The upper seismic unit is characterized by parallel-continuous seismic reflectors, that are interpreted as a succession of Pleistocene-Holocene deposits covering the erosional surface at the top of the relict prograding wedges and the Campanian Ignimbrite units (Figure 17).

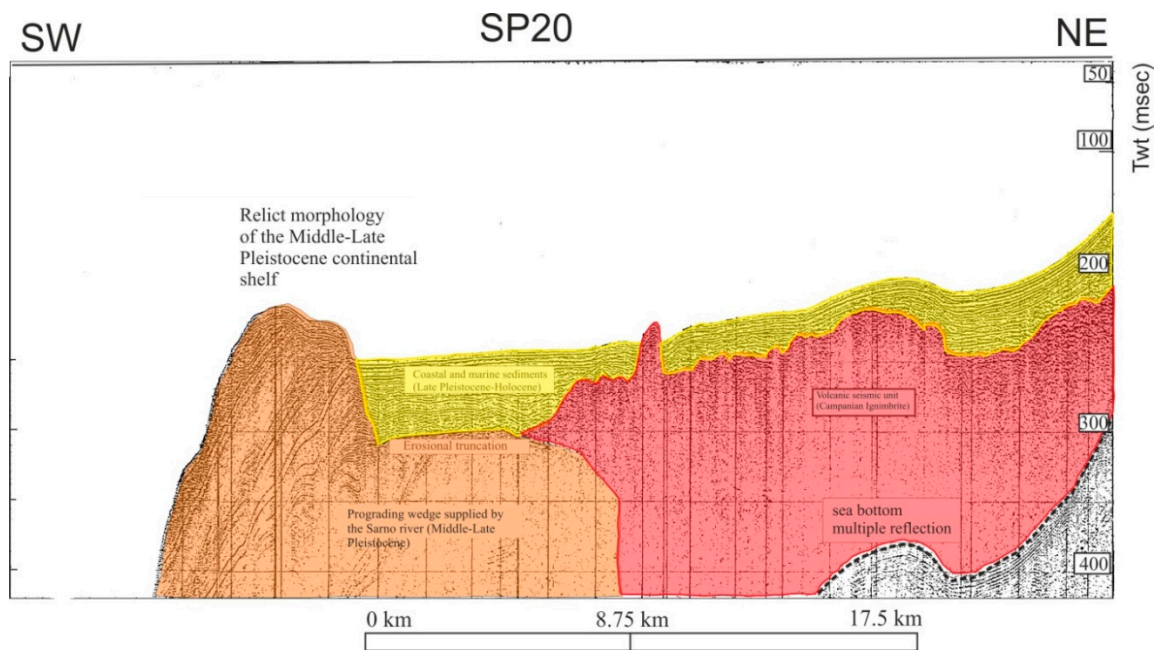


Figure 17. Geologic interpretation of the Sparker seismic profile SP20, showing the stratigraphic relationships between the relict morphologies of the Middle-Late Pleistocene continental shelf and the volcanic seismic units of the Naples Bay (Campanian Ignimbrite).

Seismic line SP20_1 illustrates the seismic stratigraphic architecture of the Naples Bay from the Banco di Fuori morpho-structural high towards the tributary channels of the Dohrn canyon (Figure 18). The seismic-stratigraphic setting of the Banco di Fuori high is characterized by the occurrence of turbiditic slope systems with mostly chaotic seismic facies, overlain by marine deposits, displaying sub-parallel reflectors, probably Late Pleistocene–Holocene in age. Tributary channels of the Dohrn canyon are incised in thick turbiditic slope systems, which form the bulk of the stratigraphic succession of the continental slope area, along with channel levee complexes (Figure 18).

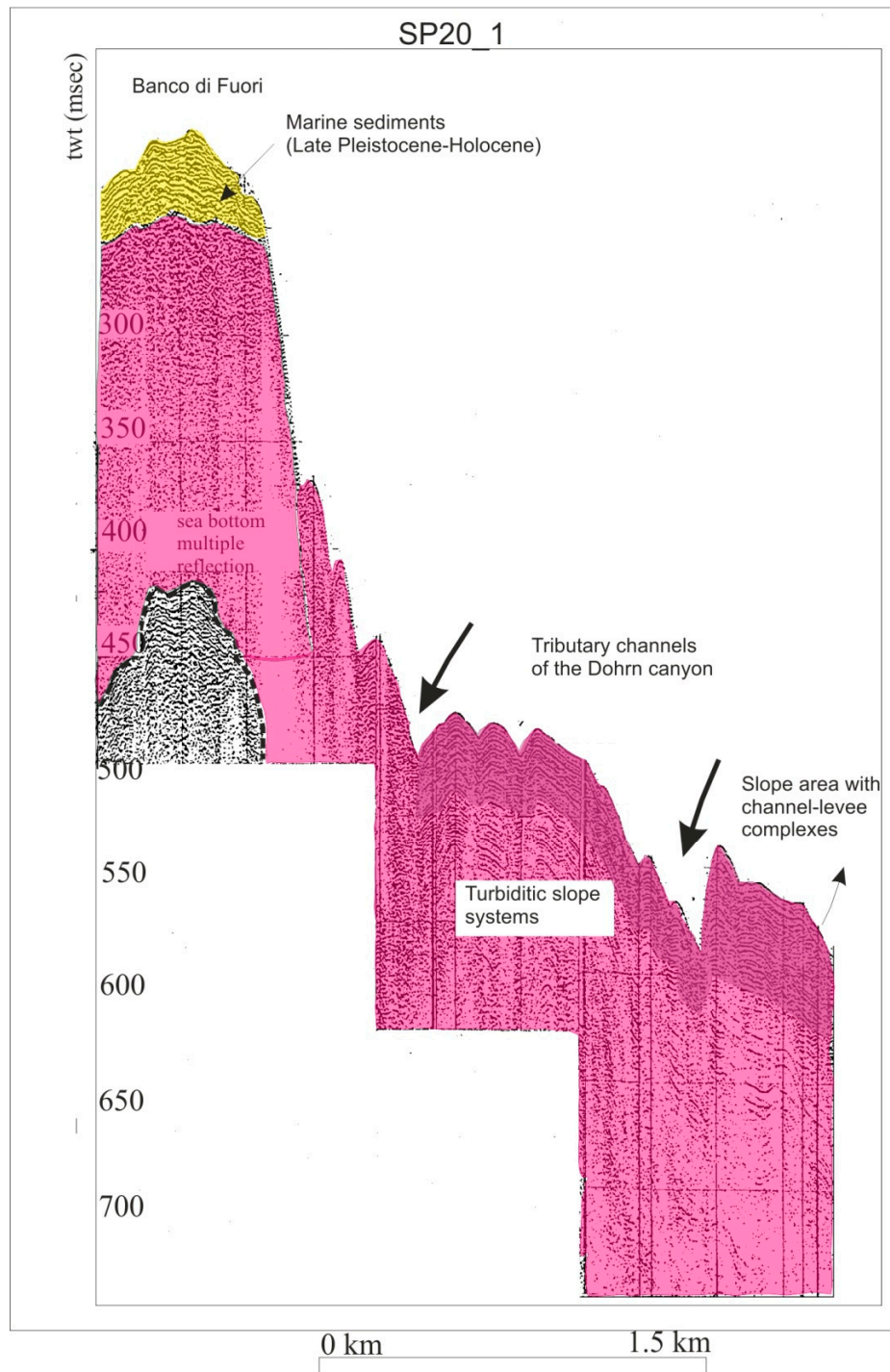


Figure 18. Geologic interpretation of the Sparker seismic profile SP20_1, exhibiting the seismo-stratigraphic setting of the Dohrn canyon next to the Banco di Fuori morpho-structural high.

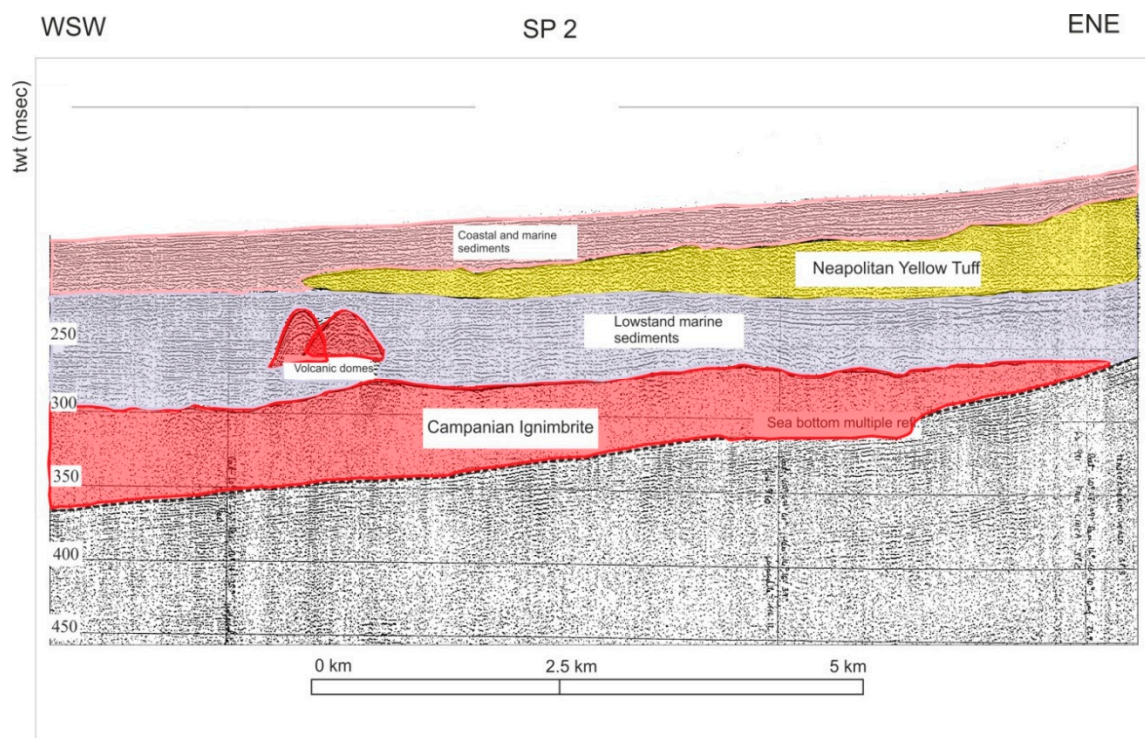


Figure 19. Geologic interpretation of the Sparker seismic profile SP2, showing the stratigraphic relationships between the volcanic seismic units of the Naples Bay (Campanian Ignimbrite and Neapolitan Yellow Tuff).

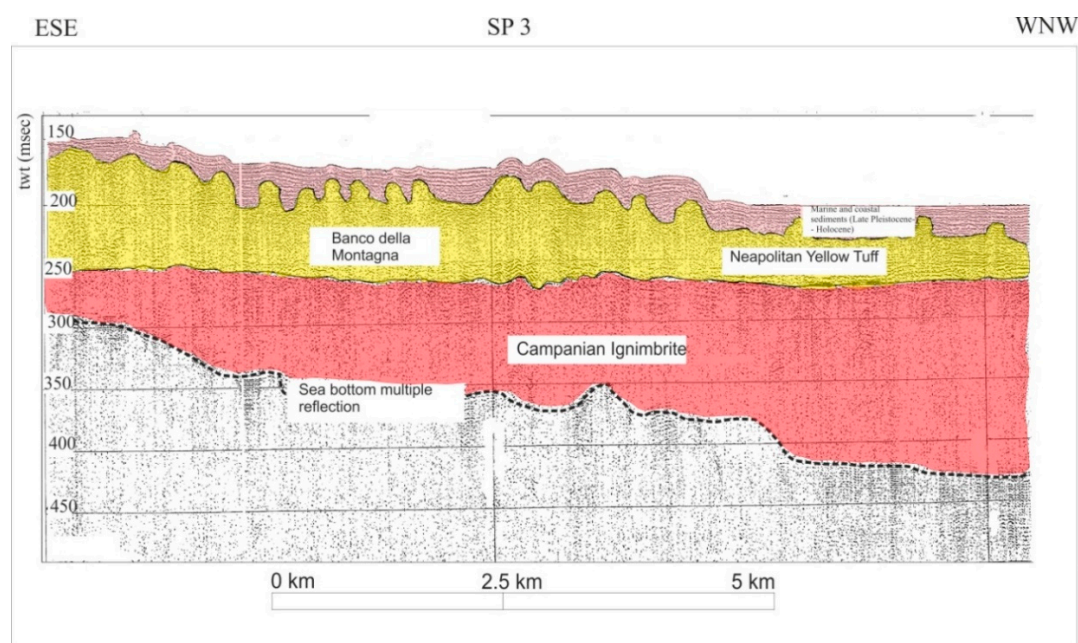


Figure 20. Geologic interpretation of the Sparker seismic profile SP3, depicting the seismo-stratigraphic setting of the volcanic seismic units of the Naples Bay in correspondence with the “Banco della Montagna” structure.

Seismic line SP2 shows the stratigraphic relationships between the volcanic seismic units of the Naples Bay; namely, the Campanian Ignimbrite (CI) and the Neapolitan Yellow Tuff (NYT). Particularly, this seismic profile highlights the occurrence of a thick marine sequence intercalated between the CI and the NYT seismic units (Figure 19). The Campanian Ignimbrite was deposited during the isotopic

stage 3 [8], whereas the Neapolitan Yellow Tuff was deposited during the upper part of the isotopic stage 2 [8] corresponding to the development of the Transgressive Systems Tract (TST) in the Naples Bay [77,110,125]. The marine sequence partly formed during the lower part of the isotopic stage 2 [8], corresponding with the Lowstand Systems Tract (LST) in the Naples Bay (Figure 19) [77,110,125,136]. Nevertheless, this unit also includes a significant volcanoclastic component, as indicated by the occurrence of volcanic domes interbedded in the LST sequence (Figure 19).

Additional information on the stratigraphic relationships between the major volcanoclastic units of the Naples Bay (namely CI and NYT) have been obtained by the Sparker seismic line SP3 (Figure 20). In this area, the lowstand deposits are missing, and the NYT unit directly overlies the CI unit. The NYT seismic unit is rooted in the Banco della Montagna structure, a wide volcanic field occurring in the Naples Bay continental shelf [81,137]. In this area the NYT unit is overlain by a succession of marine and coastal sediments, Late Pleistocene-Holocene (<15 ka) in age (Figure 20).

4.4. Sedimentological and Petrophysical Data

4.4.1. Sedimentological Data

Gravity core C74_12 has been sampled collected at water depths of 586.6 m in the lower southern part of the Dohrn western branch, close to the confluence with the Dohrn eastern branch (Figures 1 and 21). The recovered core sample displays a total length of ca 7.2 m. The core description was performed as follows, from the top (A) to the bottom by a homogeneous, bioturbated, hemipelagic mud (clayey silt and silty clay 65%) (H) of the core (Figure 21). Starting from the sea bottom, considered as a zero level a 1.5 m thick silty interbedded with coarse to very fine silty sand layers even a few decimeters thick, made of mostly volcanoclasts (pumice, scoriae, glass shards, and fragments of crystals) that probably indicate tephra layers (e), and bioclasts (forams, pteropods, ostracods, mollusks fragments) (sandy/gravelly sediments 35%) (Figure 21) bioturbated interval has been found (Figure 21). From 1.5 m to 2.8 m, massive volcanic sands interlayered with massive sandy silts occur. From 2.8 m to 4.3 m, a thick layer of volcanic sands and pumice layers, intercalated with silty layers occurs and overlies erosional surfaces, showing graded and laminated structures (Figure 21). From 4.3 m to 4.58 m, volcanic sands and pumice level interstratified with silty levels have been found (Figure 21). From 4.58 m to 5.24 m, pumice sands showing a thick pumice level have been found (Figure 21). From 5.24 m to 7.20 m, silts and sandy silts occur.

Based on a sedimentological study of the cored succession and the results of statistical grain-size analysis of the sediment, three main lithofacies associations (units) have been recognized (Figures 21 and 22). These are represented, from bottom to top by the following units [143].

- Facies A (720–530 cm)—From base to top, it consists of semi-consolidated, silty sand including lens of small, mostly rounded pumice and bioclasts with evidence of reworking. At 625 cm, a decimeter thick level of fining upward medium coarse sand, with an erosive base, consisting mainly of volcanoclasts (scoriae, minerals, and glass shards);
- Facies B (530–240 cm)—It consists of clayey silt with bioclasts (planktonic and benthonic foraminifera) interbedded with decimetric to centimetric layers and lenses of parallel and cross laminated, medium and fine sandy silt, often with erosive base and normal grading. The coarser fraction is mostly represented by gray pumice, scoriae, glass shard, well preserved minerals (e.g., sanidine, peroxide, biotite). At a depth of 530 cm, a 55 cm-thick layer of coarse pumice with sub-angular to sub-rounded clasts occurs with reverse grading (e10). Coarse-grained components of these deposits are formed by moderately sorted, sub-angular volcanoclastic fragments (pumice, scoria, K-feldspar, pyroxene, volcanic glass). These deposits pass upward to 30 cm of silty sandy pumice with rare shallow water faunas (benthic foraminifers, shell fragments). At a depth of 425 cm follows a 20 cm-thick layer, with erosional base, including sub-angular to sub-rounded pumice and occasional iron-oxidized patinas, rare pelitic pebble, and reworked fragments of Mollusk shells (e9). Toward the top follow centimetric lenses (403 cm, 378 cm, 252 cm, and 249 cm)

- and fining upward and/or parallel and crossed laminated decimetric levels (438 cm, 300 cm) of volcanoclasts, (e4–e8);
- Facies C (240–0 cm)—It is composed of homogeneous grey mud, represented by bioturbated clayey silt and clayey sandy silt with a few interbedded layers rich in volcanoclasts (170–160 cm, 160–153 cm, 43–37 cm) (e1–e3) and/or bioclasts (153–135 cm, 60–50 cm).

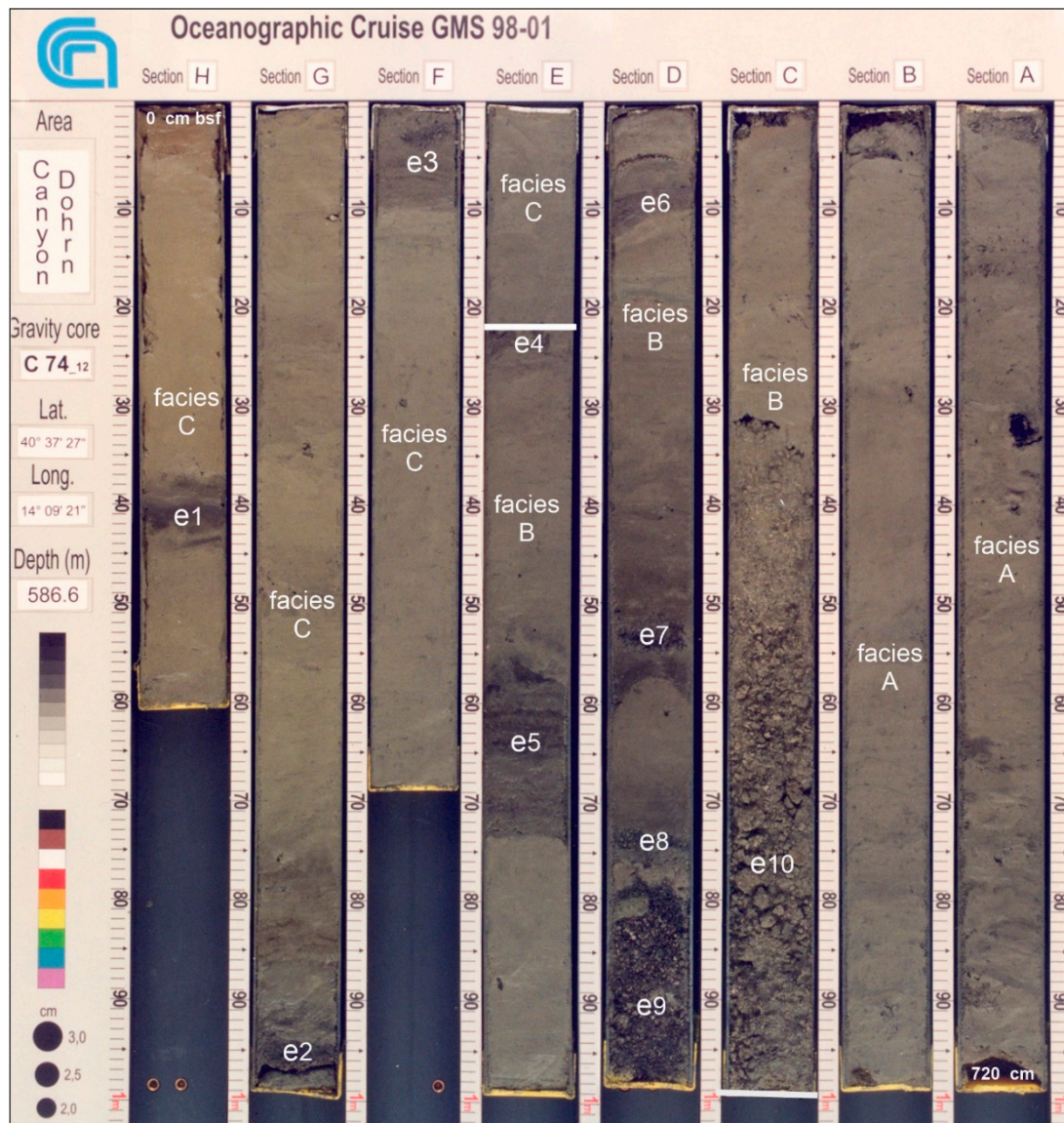


Figure 21. Sedimentologic description of the C74_12 core (Dohrn canyon).

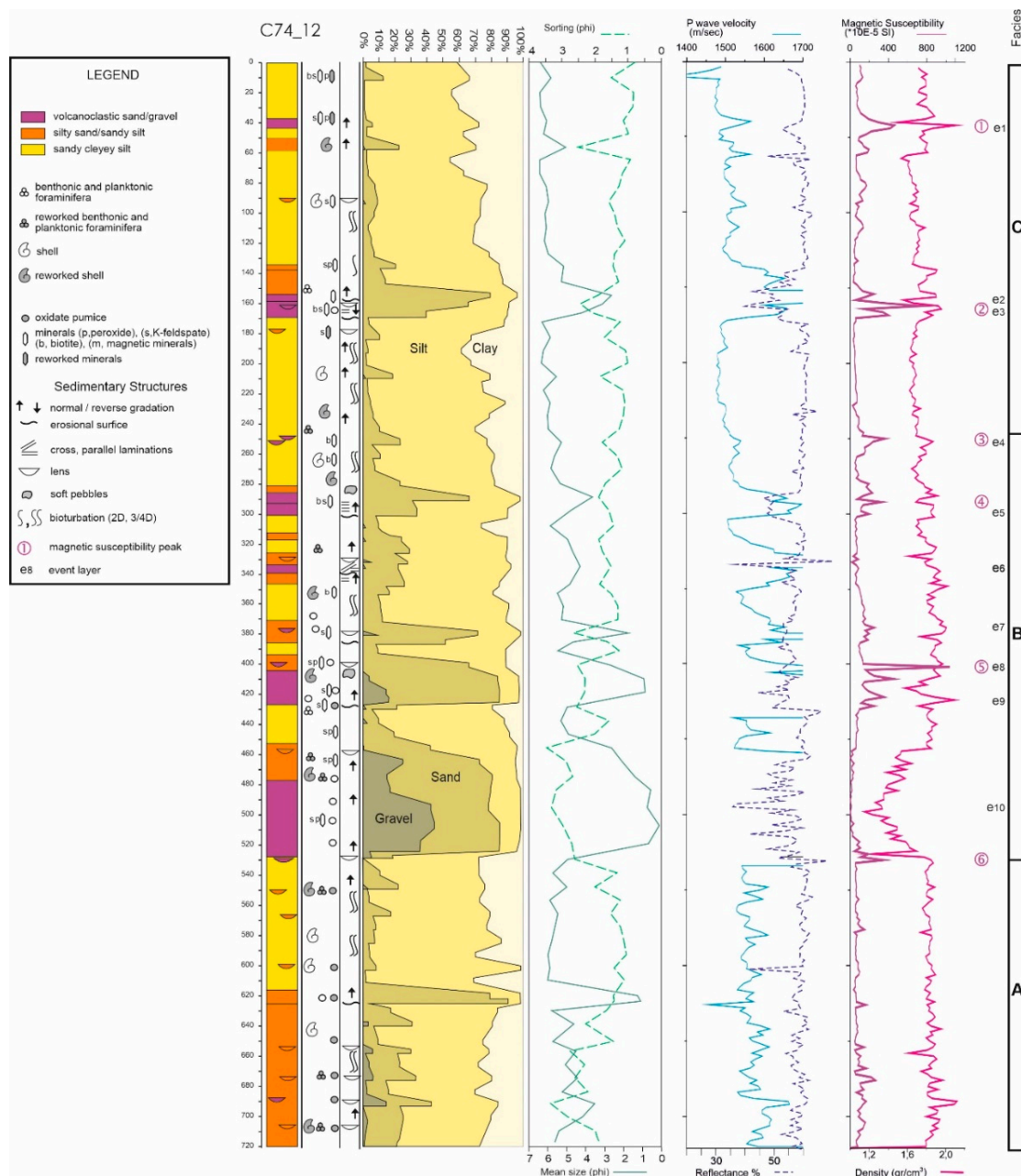


Figure 22. Integrated stratigraphy diagram of the C74_12 core (Dohrn canyon).

4.4.2. Physical Properties and Stratigraphic Correlation

The major petrophysical properties of the sampled sediments along the core logs have been analyzed in order to identify macroscopic variations and general patterns for each analyzed parameter and assist stratigraphic correlation at decimetric scale. Particular emphasis has been placed on Magnetic Susceptibility which is one of the most important parameters for the recognition of tephras and cryptotephra in mixed siliciclastic–volcaniclastic environments like the Naples Bay. Measured parameters are (1) magnetic susceptibility, (2) Gamma-ray attenuation porosity evaluator (GRAPE) density, (3) spectral reflectance, and (4) P-wave velocity. Corresponding core logs and correlation are presented in Figure 22. Continuous high-resolution (2-cm step) logs, based on measurements of physical properties of the cored sediments, have been acquired on a split-core by a fully automated Multi Sensor Core Logger (Geotek) at the petrophysical laboratory of CNR-ISMAR, Naples.

Measured parameters for the core C74_12 are: (a) magnetic susceptibility, (b) GRAPE density, (c) spectral reflectance (L%), and (d) P-wave velocity are presented in Figure 22. As a first step, the general patterns for each parameter were correlated with the lithostratigraphic log in order to identify the macroscopic facies changes at centimeter scale. Successively, the most reliable parameters for bedded siliciclastic and volcanoclastic successions (e.g., magnetic susceptibility) were analyzed in detail, trying to pinpoint single prominent peaks, as well as characteristic patterns. Finally, the preliminary parameter-based correlation was checked versus the sedimentological logs and other measured parameters.

The analysis of plot diagrams indicates that the values of volume magnetic susceptibilities display values between 2 and 1036×10^{-5} SI, with six and show six ranges (indicated by peaks 1–6) where values reach maxima between 350 and 1036×10^{-5} SI. All six peaks correlate to stratigraphic levels in which there are lithological variations with respect to embedding sediments. Particularly, peaks 1, 3, and 5 correspond to sandy silt with fine-grained pumice and scoria, with evidence of basal erosion, and representing partly reworked pyroclastic fall volcanoclastic deposits. On the other hand, peaks 4 and 6, mark normally graded, undisturbed, fine-grained pumice, and scoria sandy levels with scoria overlying muddy intervals and showing absence of erosional surface which could be interpreted as probable undisturbed volcanic sandy levels corresponding with primary pyroclastic fall deposits. Peak 2 finally appears to correlate with the base of a gravity flow deposit (e.g., grain flow/upper turbidite). Texturally homogeneous deposits (mainly composed of silts), display almost constant values of magnetic susceptibility values of volume, while the interval between 458–524 cm, which is characterized by the lowest values, consists almost exclusively of coarse pumice level of massive.

GRAPE density values swear in a range of 1.1 g/cc to 2.1 g/cm³ g/cc all along the well core. The trend pattern of variations of this parameter seems appears to follow mirror that of the trend of the magnetic susceptibility values log, including a with the main values fall remarkable minimum of (from 11.6 gr/cc to 1.1 g/cm³ gr/cc) occurring again at 458–524 cm that correlates with so far the density drop corresponds to the beginning of the above mentioned coarse pumice interval, and corresponding to the magnetic susceptibility minimum, recorded between 458 cm and 524 cm and extending all over it.

Peaks 1–6 are also distinguishable in the density record, and may yield either a positive correlation with respect to magnetic volume susceptibilities, (in the case of there is a positive correlation for peaks 1, 3, and 5), while there is an anti-parallel or anti-correlation (e.g., for peaks 2, 4, and 6) with magnetic volume susceptibility.

Spectral reflectance indicates a general trend in the variation of lower and higher values of the change in sediment's lightness, and particularly interesting is to note that it shows a tendency to correlation with the variation of lower and higher trend values in correspondence of magnetic susceptibility peaks, which could indicate a relative abundance between darker or/and lighter volcanic sediments depending by their different contents (e.g., (pumices/sandine or scoriaceous/lithics enrichment).

Finally, it should be noted that the quality of the P-wave velocity log data is not fully recorded, not due to the partial loss of signal (the signal is lost, perhaps as a consequence of the presence of voids, in the coarse-grained volcanoclastic interval). On the other hand, where the signal was well recorded within intervals 0–400 cm and 540–720 cm, it is interesting to note that where the trend of the variations is similar to that one of the density log, particularly between 180 cm and 340 cm the P-wave velocity peaks 3 (1538 m/s) and 4 (maximum speed 1538 m/s and 1694 m/s respectively) seem to correspond to a fair correlation with GRAPE density maxima. Continuous high-resolution logs based on physical properties measurements of the cores have been acquired on a split-core by a fully automated Multi Sensor Core Logger (Geotek) at the CNR-ISMAR of Naples (Italy) petrophysical laboratory. The measured parameters are the magnetic susceptibility, the GRAPE density, the compressional P-wave velocity, and the spectral reflectance.

5. Discussion

Submarine canyons represent important erosive lineaments of the seafloor morphology. They deeply cut long belts of the continental slopes and provide a main mode for the transfer of coastal sediments mode through which both siliciclastic and volcanoclastic materials coming from the coastal zones are transported towards the deep oceanic basins. Previous research on Neogene evolution of the main continental margins of the Mediterranean, North Atlantic and Pacific areas has confirmed the common occurrence of large palaeo-channels, often inter-layered in the Quaternary deposits of the sedimentary basins, suggesting that the origin of these kinds of canyons could be genetically related with the subaerial environment [56,144–150].

The main parameters in the study of submarine canyons include (a) the depth range, (b) the slope gradient, (c) the relationships between canyon morphology and tectonic lineaments, (d) the shape of canyon section, i.e., U-shape (depositional) and V-shape (erosive), and (e) the canyon profile (rectilinear or meandering) [56].

Several studies on the Dohrn canyon have been carried out during the last decades, mostly regarding the distribution of volcanic centers of the Naples Bay area and regional tectonic lineaments, as well as the seismic stratigraphic architecture of the continental margin of the Campania region and associated depositional environments offshore [77,78,138,151,152]. Other research has focused on the morpho-bathymetric setting of the Dohrn and Magnaghi canyons and submarine gravity instabilities [81,137] and the potential run-up and tsunami reconstruction from fossil submarine landslides [79].

Previous studies have suggested that, in the submarine sector of the Naples Bay the deposition of thick volcanic units (CI and NYT) was coeval with the formation of the Dohrn canyon, suggesting this process was acting during the eustatic sea level fall and the tectonic uplift of the outer shelf domains during the Late Quaternary [77]. Other authors have proposed that the Dohrn and the Magnaghi canyons may be related to a much older, inherited drainage system genetically linked to the latest Neogene-Pleistocene tectonic evolution of the Campania continental margin [151,152].

The Magnaghi canyon and the Dohrn western branch show morphological indication of retreating canyon heads. This evidence is essential for the understanding of the submarine canyon formation, since the sediment flows may have repeatedly triggered retrogressive failures, according to the commonly accepted models on submarine canyon evolution [54]. The process of canyon formation can be interpreted by reconciling morphological evidence for headward canyon erosion by mass wasting with the stratigraphic evidence for canyon inception by downslope-eroding sediment flows. The canyon morphology and evolution could be summarized by hypothesizing a scenario from “youthful” to “mature” canyon morphology [64]. The youthful stage of submarine canyon evolution begins with extensive slope failures. Retrogressive mass wasting of continental slope sediments along the failure headwall leads to the formation and upslope extension of relatively straight, steep-walled chute. If this headward migrating chute breaches the shelf break, the canyon taps into a new sediment source of outer shelf sands and enters into a mature phase of canyon evolution. The failure of shelf sediments in the vicinity of the canyon head initiates coarse-grained gravity flow processes (e.g., turbidity currents, debris/grain flows), which become an important agent in canyon erosion by downcutting the canyon and creating a sinuous thalweg [54,64].

Previous interpretations have reported that there is no evidence of a high sediment supply along the shelf edge of the Naples Bay during the Late Quaternary, as the sediment originating from the emerged areas was possibly deposited on the continental shelf, as a consequence of tectonic subsidence [77]. The results of our study indicate, on the contrary, that during the late Pleistocene sediment supply (particularly volcanoclastic input) was extremely high in the area, due to the eruption of the Campanian Ignimbrite (CI) and the Neapolitan Yellow Tuff (NYT). Moreover, the considerable amount of available sediment also played a major role in the building of the stratigraphic architecture of the Naples Bay and the formation of the canyon system.

The stratigraphic analysis of gravity core C74_12 documents a succession of primary and mostly reworked tephra layers interbedded with hemipelagic deposits. Tephra layers ostensibly represent periods of significant volcanoclastic input and sediment transport along the axis of the Dohrn canyon, whereas hemipelagic intervals (i.e., bioturbated mud) denote phases of quiescence of sediment transport throughout the canyon. Volcanoclastic input mainly consists of sediment gravity flows (e.g., turbidite and debris/grain flow), likely originated in the upper part of the canyon from massive accumulation of primary pyroclastic deposits on the outer shelf and upper slope of the Naples Bay that become mixed with hemipelagic material during the sedimentary transport downslope (e.g., facies C, layers e2 and e3; facies B, layers e9 and e10) (Figures 21 and 22). In some cases, gravity flow deposits stack up one upon another, suggesting the occurrence of periods of enhanced activity in sediment transport and a high frequency of re-sedimentation processes.

A thin drape of hemipelagic sediments, detected on seismic profiles and confirmed by sedimentological analysis, appears to cover the whole Dohrn canyon system, suggesting a substantial present-day inactivity of the Dohrn canyon, likely as a consequence of the recent decrease of volcanoclastic input into the Naples Bay and the concomitant high sea level stillstand. In core C74_12 the recent phase of quiescence of the Dohrn canyon is evidenced by ca. 1.5 m thick interval of bioturbated silt (hemipelagite) immediately beneath the seafloor (Figure 21).

Our interpretation confirms the suggestion that the Dohrn canyon is genetically related with the main eruptive events involving the Naples Bay during the latest Pleistocene, including the CI; (ca. 39 ka B.P.) [21] and the NYT (ca. 15 ky B.P.) [75], recently correlated with main tephra levels occurring in the Northern Campi Flegrei offshore [76]. The significant volcanoclastic supply during the eruptive phases occurring in the Neapolitan area during this period has probably controlled the individuation of the Dohrn canyon western branch. Similarly, we infer that the individuation of the Dohrn eastern branch occurred by the joining of a paleo-valley located offshore the Sorrento Peninsula, likely as a consequence of high sedimentary supply from the Schiazzano river mouth [77].

The results of our research are in agreement with the geological model recently presented for the Pozzuoli Bay by Steinmann et al. (2018) [33], which includes a scenario for the formation of the Dohrn canyon. Based on this model a possible kinematic reconstruction of the northern part of the Naples Bay during the last 15 ka, can be summarized into five main stages (Figures 23 and 24). The paleo-coastlines for each stage have been inferred through an integrated analysis of seismic and bathymetric data [78], onshore outcrops [20], and borehole stratigraphic columns [20,21].

- Stage 1 (15 ka) During stage 1 the sea level stationed at ca. −93 m below the present-day level and the main volcano-tectonic event was represented by the caldera collapse related to the NYT eruption (Figures 23 and 24). The central part of the NYT caldera collapse was in the submarine domain, whereas outside of the caldera depression, subaerial conditions prevailed in the coastal area. Unconformity U2 correlates with the top of the NYT deposits and represents a partly submarine and partly subaerial feature. This unconformity also marks a channel-like topographic low, genetically related with the erosional truncation of the M1 seismic sequence (Figure 24), corresponding to the actual location of the Dohrn Canyon and its continuation toward the north-west. The Miseno bank was partly emerged, and formed a peninsula connected to the mainland, whereas the Pentapalumbo bank was an island in northern Naples Bay. During this stage, the Dohrn canyon extended toward the north-west and drained significant amounts of volcanoclastic materials originated during the NYT eruption toward the outer shelf and slope.
- Stage 2 (15.0–8.6 ka) During stage 2, the sea level rose to ca. 19 m below the present-day level, causing a generalized backstepping of depositional systems and the flooding of the Miseno and Pentapalumbo banks. During this period (10.3–9.5 ka) the tuff cone of Nisida Bank, was formed. At the Dohrn canyon head, the onset of this tuff cone had the effect of hampering the down-canyon removal of volcanoclastic deposits, which resulted in turn in a rapid infilling of the abandoned section of the canyon (DC = Dohrn canyon fill). During the sea level rise prograding clinofolds developed on the flanks of the bathymetric highs of the Miseno and Pentapalumbo banks.

- Stage 3 (8.6–5.0 ka) During stage 3, the sea level rose from ca. 19 m to 4 m below the present-day level (Figures 23 and 24) and at least six magmatic to phreato-magmatic eruptions occurred. The sea level rise resulted in additional landward retreat of the shoreline outside of the NYT caldera structure. Early during this stage the La Starza terrace (Pozzuoli Bay) progressively emerged due to the ground uplift associated with the NYT caldera resurgence and, at same time, marine unconformities U3 and U4 formed as a response to the consequent decrease in the accommodation space over the continental shelf (Figures 23 and 24).
- Stage 4 (5.0–2.0 ka) Stage 4 represents a period of minor sea level rise, from 4 m to 1 m below the present-day sea level, that was accompanied by a further backstepping of depositional systems and landward shift of the shoreline. At the time of the eruptions of Capo Miseno (3.7 ka B.P.) and Nisida Island (3.98 ka B.P.), sea level was 2.5–2.7 m below the present-day level. The deposits of both these eruptions are found, as reworked marine tephra layers in the stratigraphic record of the Pozzuoli Bay and can be used as chronostratigraphic markers. Marine unconformity U5 marks the end of the uplift phase associated with last major eruptions occurred in the marine area of the Campi Flegrei and postdates the tephra layers resulted from the events of Capo Miseno and Nisida Island (Figures 23 and 24).
- Stage 5 (2.0 ka–present) During stage 5, the sea level slightly continued to rise from ca. –1 m to the present the present-day level (Figures 23 and 24). Since the beginning of this stage a significant phase of subsidence, affected the inner sector of the Pozzuoli Bay as testified by dramatic drowning of coastal settlements and infrastructures of Roman age. Subsidence in the range of 20 m to 8 m, with average rates of 10–4 mm/year also led to the drowning of the coastal shallow-water terrace associated with unconformity U6 and related prograding clinofolds. This created significant accommodation space, resulting in the deposition of the present day coastal prograding wedge (Figure 23).

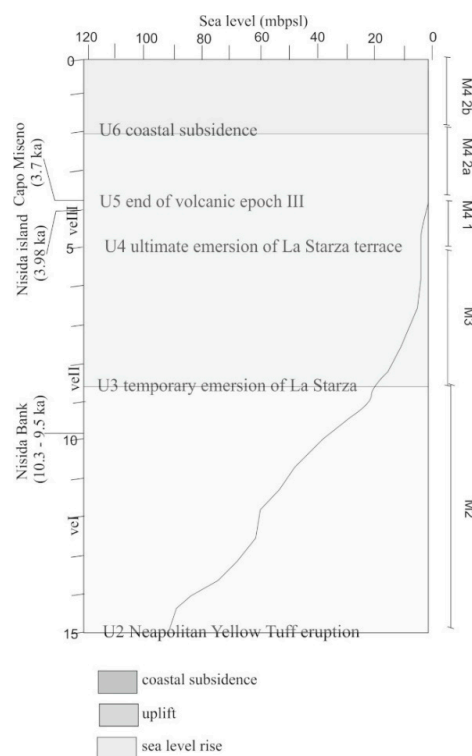


Figure 23. Graphical summary of main depositional units (Seismic Units M2–M4.2) and stratigraphic markers (Unconformities U2–U6) shown in Figure 24, in correlation with sea-level rise and the prevailing depositional environment (modified after Steinmann et al., 2018) [33]. The relative sea-level curve was adapted from Lambeck et al. (2011).

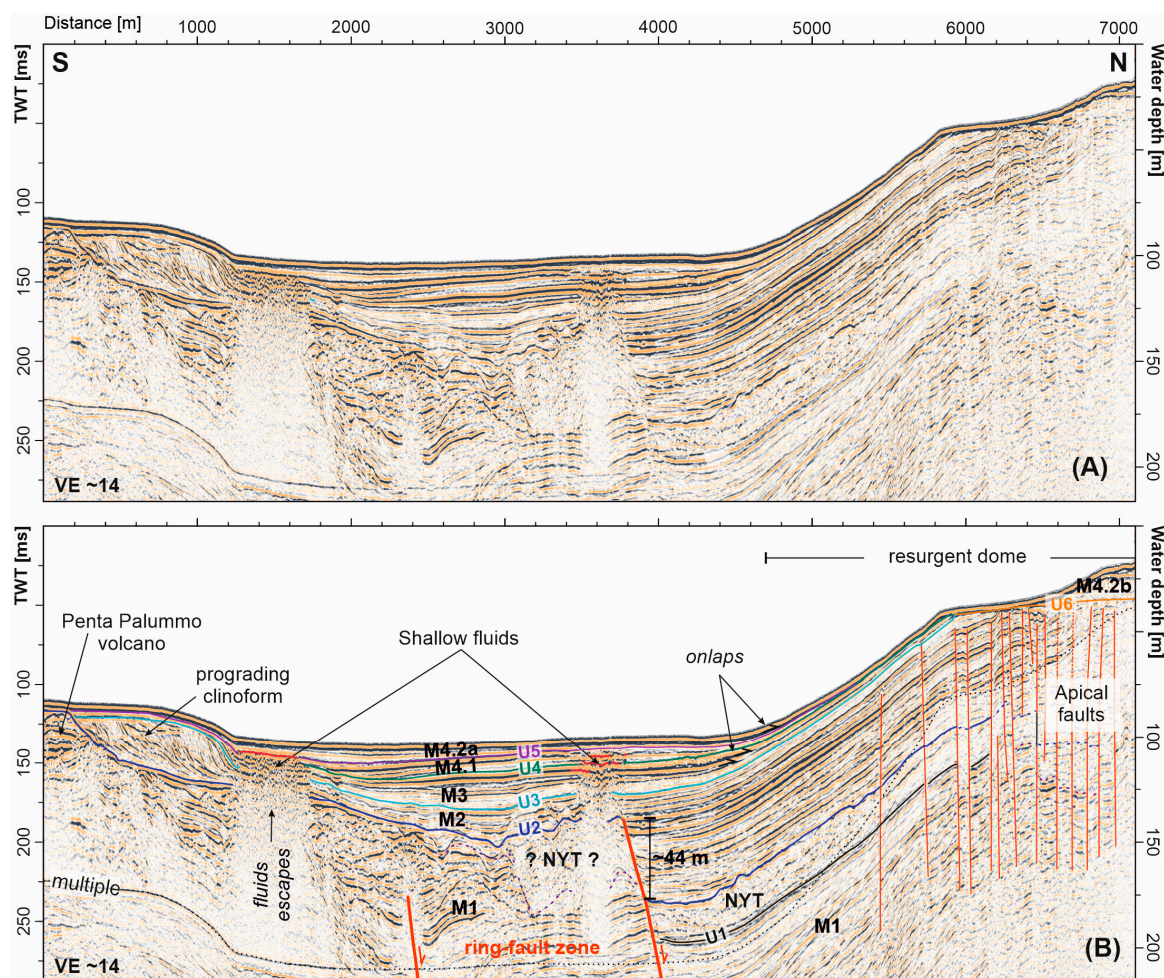


Figure 24. Uninterpreted (A) and interpreted (B) seismic profile GeoB08-045 (modified after Steinmann et al., 2018) [33], showing the main marine units and the corresponding regional unconformities (U2–U6), that correlate with the main volcano-tectonic events (see Figure 23).

6. Conclusions

Two deeply incised canyons drain the continental shelf and the upper slope of the Bay of Naples (Southern Italy), an active volcanic area since Middle-Late Pleistocene. Erosion and transport of volcanoclastic sediments from the Campi Flegrei and Procida Island have acted mainly along the Magnaghi canyon and the Dohrn western branch, whereas a consistent fluvial supply coming from the Sarno river fed the Dohrn eastern branch. The Magnaghi trilobate canyon head displays retrogressive failures engraving the continental shelf. Sedimentary processes are dominated by gravity flows (turbidite and debris/grain flows) mostly moving downslope toward the southwest due to the local control of a morpho-structural high represented by Meso-Cenozoic basement rocks.

Based on the results of seismic stratigraphic interpretation, the Dohrn canyon is definitely older than the volcanic deposits of the Neapolitan Yellow Tuff (NYT) (ca. 15 ka B.P.) that form the backbone of the town of Naples [21,75].

The walls of Dohrn canyon were affected by slope failures mostly along the western flanks, where large slide scars occur. Material displaced by slope failure processes was effectively removed and redistributed toward the southeast by dominant gravity flows (turbidite and debris/grain flows). Sedimentological analysis of gravity core C74_12 revealed the occurrence, along the axis of Dohrn canyon of reworked, K-feldspar-rich pumiceous tephra layers and volcanoclastic gravity flow deposits interbedded with bioturbated muddy intervals (hemipelagite) marking phases of quiescence in the canyon activity. Gravity flow processes were accompanied by the overflow of sediment spills over

levees of tributary channels, producing overbank deposits along the canyon sides. Fossil tributary channels suspended over the main branches testify for phases of rapid re-incision switching off the feeding from lateral sources. A thin drape of hemipelagic muddy sediments covering the whole canyon system, suggests its present-day inactivity, probably due to the decreasing volcanoclastic supply and to the high sea-level stillstand.

The instability phenomena documented along the Dohrn canyon slopes may be interpreted as the result of a phases of rapid accumulation of volcanoclastic deposits on the continental shelf due to (a) climatically induced enhanced erosion and associated high sediment input in the Bay of Naples or (b) the deposition of large volumes of volcanoclastic sediments as a consequence of massive volcanoclastic input into the coastal sedimentary environment of the Naples Bay during the Late Pleistocene. Seismic stratigraphic interpretation calibrated with the sedimentological analysis of gravity core samples suggests an upper fan valley–levee depositional setting for this stratigraphic interval.

Author Contributions: G.A. and M.S. wrote the paper, processed and interpreted the seismic and morpho-bathymetric data and constructed the figures. F.M. described the core C74_12 and interpreted the sedimentological data. G.A. and M.I. correlated the sedimentological data with the petrophysical data. M.I. recorded the petrophysical data. M.S. constructed the model of Figure 23 and interpreted the seismic sections in Figure 24. G.A. reviewed the first, the second, the third, the fourth, and the fifth versions of the manuscript. M.S. reviewed the fifth version of the manuscript. All authors have read and agreed to the published version of the manuscript.

Funding: This research was funded by the National Research Council of Italy, by the ISPRA Agency (Rome, Italy), and by the Region Campania (Sector of Soil Defense, Geothermics and Geotechnics, Naples, Italy).

Acknowledgments: The data presented in this study were acquired by CNR-ISMAR, Napoli within the frame of a national project (CARG) for the geological mapping of Italy at 1:50,000, funded by ISPRA (Rome, Italy) and Regione Campania (Naples, Italy). We thank our colleague Antimo Angelino for his support in the acquisition of the petrophysical core logs at the CNR-ISMAR laboratories. We thank three anonymous reviewers for their comments that greatly improved the early version of the manuscript.

Conflicts of Interest: The authors declare no conflict of interest.

References

1. Fabbri, A.; Gallignani, P.; Zitellini, N. Geologic evolution of the peri-Tyrrhenian sedimentary basins. In *Sedimentary Basins of Mediterranean Margins*, 1st ed.; Wezel, F.C., Ed.; Tecnoprint: Bologna, Italy, 1981; pp. 101–127.
2. Malinverno, A.; Ryan, W.B.F. Extension in the Tyrrhenian sea and shortening in the Apennines as a result of arc migration driven by sinking of the lithosphere. *Tectonics* **1986**, *5*, 227–245. [[CrossRef](#)]
3. Trincardi, F.; Zitellini, N. The rifting of the Tyrrhenian basin. *Geomarine Lett.* **1987**, *7*, 1–6. [[CrossRef](#)]
4. Oldow, J.S.; D’Argenio, B.; Ferranti, L.; Pappone, G.; Marsella, E.; Sacchi, M. Large-Scale longitudinal extension in the southern Apennines contractional belt. *Geology* **1993**, *21*, 1123–1126. [[CrossRef](#)]
5. Shackleton, N.J.; Opdyke, N.D. Oxygen isotope and palaeomagnetic stratigraphy of equatorial Pacific core V28-238: Oxygen isotope temperatures and ice volume on a 10⁵ and 10⁶ year scale. *Quat. Res.* **1973**, *3*, 39–55. [[CrossRef](#)]
6. Fairbanks, R.G.; Matthews, R.K. The marine oxygen isotope record in Pleistocene coral, Barbados, West Indies. *Quat. Res.* **1978**, *10*, 181–196. [[CrossRef](#)]
7. Chappell, J.; Shackleton, N.J. Oxygen isotopes and sea level. *Nature* **1986**, *324*, 137–140. [[CrossRef](#)]
8. Martinson, D.G.; Pisias, N.G.; Hays, J.D.; Imbrie, J.S.; Moore, T.C.; Shackleton, N.J. Age Dating and the Orbital Theory of the Ice Ages: Development of a High Resolution 0 to 300,000 year chronostratigraphy. *Quat. Res.* **1987**, *27*, 1–29. [[CrossRef](#)]
9. Bard, E.; Hamelin, B.; Fairbanks, R.G. U-Th ages obtained by mass spectrometry in corals from Barbados: Sea level during the past 130,000 years. *Nature* **1990**, *346*, 456–458. [[CrossRef](#)]
10. Pirazzoli, P.A. Global sea-level changes and their measurements. *Glob. Planet. Chang.* **1993**, *8*, 135–148. [[CrossRef](#)]
11. Lambeck, K.; Chappell, J. Sea level change through the Last glacial cycle. *Science* **2001**, *292*, 679–686. [[CrossRef](#)]

12. Mastronuzzi, G.; Sansò, P.; Murray-Wallace, C.V.; Shennan, I. Quaternary coastal morphology and sea level changes—An introduction. *Quat. Sci. Rev.* **2005**, *21*, 283–293. [[CrossRef](#)]
13. Caputo, R. Sea-level curves: Perplexities of an end-user in morphotectonic applications. *Glob. Planet. Chang.* **2007**, *57*, 417–423. [[CrossRef](#)]
14. Gamberi, F.; Marani, M. Deep-sea depositional systems of the Tyrrhenian basin. *Mem. Descr Carta Geol. d'Ital.* **2004**, *54*, 127–146.
15. Cosentino, D.; De Rita, D.; Funiciello, R.; Parotto, M.; Salvini, F.; Vittori, E. Fracture System in Phlegrean Fields (Naples, Southern Italy). *Bull. Volcanol.* **1984**, *47*, 247–257. [[CrossRef](#)]
16. Di Girolamo, P.; Ghiara, M.R.; Lirer, L.; Munno, R.; Rolandi, G.; Stanzione, D. Vulcanologia e petrologia dei Campi Flegrei. *Boll. Della Soc. Geol. Ital.* **1984**, *103*, 349–413.
17. Cinque, A.; Rolandi, G.; Zamparelli, V. L'estensione dei depositi marini olocenici nei Campi Flegrei in relazione alla vulcano tettonica. *Boll. Della Soc. Geol. Ital.* **1985**, *104*, 327–348.
18. Rosi, M.; Sbrana, A. *Phlegrean Fields*; Quaderni De La Ricerca Scientifica, Consiglio Nazionale delle Ricerche: Roma, Italy, 1987; Volume 114, pp. 1–175.
19. Scandone, R.; Bellucci, F.; Lirer, L.; Rolandi, G. The structure of the Campanian Plain and the activity of the Neapolitan Volcanoes (Italy). *J. Volcanol. Geotherm. Res.* **1991**, *48*, 1–31. [[CrossRef](#)]
20. Orsi, G.; De Vita, S.; Di Vito, M.A. The restless, resurgent Campi Flegrei nested caldera (Italy): Constraints on its evolution and its configuration. *J. Volcanol. Geotherm. Res.* **1996**, *74*, 179–214. [[CrossRef](#)]
21. Di Vito, M.A.; Isaia, R.; Orsi, G.; Southon, J.; De Vita, S.; D'Antonio, M.; Pappalardo, L.; Piochi, M. Volcanic and deformational history of the Campi Flegrei caldera in the past 12 ka. *J. Volcanol. Geotherm. Res.* **1999**, *91*, 221–246. [[CrossRef](#)]
22. Perrotta, A.; Scarpati, C.; Luongo, G.; Morra, V. The Campi Flegrei caldera boundary in the city of Naples. In *Volcanism in the Campania Plain: Vesuvius, Campi Flegrei and Ignimbrites*, 1st ed.; De Vivo, B., Ed.; Elsevier Science Publishers: Amsterdam, The Netherlands, 2006; pp. 85–96.
23. Acocella, V.; Funiciello, R.; Marotta, E.; Orsi, G.; De Vita, S. The role of extensional structures on experimental calderas and resurgence. *J. Volcanol. Geotherm. Res.* **2004**, *129*, 199–217. [[CrossRef](#)]
24. Acocella, V. Activating and reactivating pairs of nested collapses during caldera forming eruptions: Campi Flegrei, Italy. *Geophys. Res. Lett.* **2008**, *35*, L17304. [[CrossRef](#)]
25. Acocella, V. Evaluating fracture patterns within a resurgent caldera: Campi Flegrei, Italy. *Bull. Volcanol.* **2010**, *72*, 623–638. [[CrossRef](#)]
26. Costa, A.; Folch, A.; Macedonio, G.; Giaccio, B.; Isaia, R.; Smith, V.C. Quantifying volcanic ash dispersal and impact of the Campanian Ignimbrite super-eruption. *Geophys. Res. Lett.* **2012**, *39*. [[CrossRef](#)]
27. Capuano, P.; Russo, G.; Civetta, L.; Orsi, G.; D'Antonio, M.; Moretti, R. The active portion of the Campi Flegrei caldera structure imaged by 3-D inversion of gravity data. *Geochem. Geophys. Geosyst.* **2013**, *14*. [[CrossRef](#)]
28. Sacchi, M.; Pepe, F.; Corradino, M.; Insinga, D.D.; Molisso, F.; Lubritto, C. The Neapolitan Yellow Tuff caldera offshore the Campi Flegrei: Stratal architecture and kinematic reconstruction during the last 15 ky. *Mar. Geol.* **2014**, *354*, 15–33. [[CrossRef](#)]
29. Vitale, S.; Isaia, R. Fractures and faults in volcanic rocks (Campi Flegrei, Southern Italy): Insight into volcano-tectonic processes. *Int. J. Earth Sci.* **2014**, *103*, 801–819. [[CrossRef](#)]
30. Aiello, G.; Marsella, E.; Di Fiore, V. New seismo-stratigraphic and marine magnetic data of the Gulf of Pozzuoli (Naples Bay, Tyrrhenian Sea, Italy): Inferences for the tectonic and magmatic events of the Phlegrean Fields volcanic complex. *Mar. Geophys. Res.* **2012**, *33*, 93–125. [[CrossRef](#)]
31. Aiello, G.; Giordano, L.; Giordano, F. High resolution seismic stratigraphy of the Gulf of Pozzuoli (Naples Bay) and relationships with submarine volcanic setting of the Phlegrean Fields volcanic complex. *Rend. Lincei* **2016**, *27*, 775–801. [[CrossRef](#)]
32. Steinmann, L.; Spiess, V.; Sacchi, M. The Campi Flegrei caldera (Italy): Formation and evolution in interplay with sea level variations since the Campanian Ignimbrite eruption at 39 ka. *J. Volcanol. Geotherm. Res.* **2016**, *327*, 361–374. [[CrossRef](#)]
33. Steinmann, L.; Spiess, V.; Sacchi, M. Post-collapse evolution of a coastal caldera system: Insight from a 3D multichannel seismic survey from the Campi Flegrei caldera (Italy). *J. Volcanol. Geotherm. Res.* **2018**, *349*, 83–98. [[CrossRef](#)]

34. Cassano, E.; La Torre, P. Geophysics. In *Somma-Vesuvius*; Santacroce, R., Ed.; Consiglio Nazionale delle Ricerche: Roma, Italy, 1987; pp. 175–195.
35. Santacroce, R. *Somma-Vesuvius*; Consiglio Nazionale delle Ricerche: Rome, Italy, 1987; pp. 1–251.
36. Esposti Ongaro, T.; Neri, A.; Todesco, M.; Macedonio, G. Pyroclastic flow hazard at Vesuvius from numerical modelling II. Analysis of local flow variables. *Bull. Volcanol.* **2002**, *64*, 178–191. [[CrossRef](#)]
37. Mastrolorenzo, G.; Palladino, D.; Vecchio, G.; Taddeucci, J. The 472 AD Pollena eruption of Somma-Vesuvius (Italy) and its environmental impact at the end of Roman Empire. *J. Volcanol. Geotherm. Res.* **2002**, *113*, 19–36. [[CrossRef](#)]
38. Saccorotti, G.; Ventura, G.; Vilardo, G. Seismic swarms related to diffusive processes: The case of Somma-Vesuvius volcano, Italy. *Geophysics* **2002**, *67*, 199–203. [[CrossRef](#)]
39. Scarpa, R.; Tronca, F.; Bianco, F.; Del Pezzo, E. High resolution velocity structure beneath Mount Vesuvius from seismic array data. *Geophys. Res. Lett.* **2002**, *29*, 2040. [[CrossRef](#)]
40. Cioni, R.; Bertagnini, A.; Santacroce, R.; Andronico, D. Explosive activity and eruption scenarios at Somma-Vesuvius (Italy): Towards a new classification scheme. *J. Volcanol. Geotherm. Res.* **2009**, *178*, 331–346. [[CrossRef](#)]
41. D’Auria, L.; Massa, B.; De Matteo, A. The stress field beneath a quiescent stratovolcano: The case of Mount Vesuvius. *J. Geophys. Res. Solid Earth* **2014**, *119*, 1181–1199. [[CrossRef](#)]
42. La Rocca, M.; Galluzzo, D. Seismic monitoring at Mt. Vesuvius by array methods. *Seismol. Res. Lett.* **2014**, *85*, 809–816. [[CrossRef](#)]
43. Luongo, G.; Civetta, L.; Gasparini, P.; Macedonio, G. Vesuvio: La storia dei piani di protezione civile. *L’Ambiente Antrop. Territ. Città Archit.* **2014**, *3*, 6–25.
44. Avanzinelli, R.; Cioni, R.; Conticelli, S.; Giordano, G.; Isaia, R.; Mattei, M.; Sulpizio, R. Guida all’escursione pre-meeting “The Vesuvius and the other Volcanoes of central Italy”. *Goldschmidt* **2013**, *2017*, 25–30. [[CrossRef](#)]
45. Brown, L.F.; Fisher, W.L. Seismic stratigraphic interpretation of depositional systems. Examples from Brazilian rift and pull-apart basins. In *Seismic Stratigraphy: Applications to Hydrocarbon Exploration*; Payton, C.E., Ed.; American Association of Petroleum Geologists: Tulsa, OK, USA, 1977; Volume 26, pp. 213–248.
46. Bouma, A. *Sedimentology of Some Flysch Deposits: A Graphic Approach to Facies Interpretation*; Elsevier Science Publishers: Amsterdam, The Netherlands, 1962; pp. 1–168.
47. Kenyon, N.H. Mass wasting features on the continental slope of northwest Europe. *Mar. Geol.* **1987**, *74*, 57–77. [[CrossRef](#)]
48. Bugge, T.; Belderson, R.H.; Kenyon, N.H. The Storegga Slide. *Philos. Trans. R. Soc.* **1988**, *325*, 357–388.
49. Soh, W.; Tokuyama, H.; Fujoka, K.; Kato, S.; Taira, A. Morphology and development of a deep-sea meandering canyon (Boso Canyon) on an active plate margin. *Mar. Geol.* **1990**, *91*, 227–241. [[CrossRef](#)]
50. Ergin, M.; Bodur, M.N.; Ediger, V. Distribution of surficial shelf sediments in the northeastern and southeastern parts of the Sea of Marmara Strait and canyon regimes of the Dardanelles and Bosphorus. *Mar. Geol.* **1991**, *96*, 313–340. [[CrossRef](#)]
51. Ediger, V.; Okyar, M.; Ergin, M. Seismic stratigraphy of the fault-controlled submarine canyon/valley system on the shelf and upper slope of the Anamur Bay, Northeastern Mediterranean Sea. *Mar. Geol.* **1993**, *115*, 129–142. [[CrossRef](#)]
52. Hagen, R.A.; Bergersen, D.D.; Moberly, R.; Coulbourn, W.T. Morphology of a large meandering submarine canyon system on the Peru-Chile forearc. *Mar. Geol.* **1994**, *119*, 7–38. [[CrossRef](#)]
53. Hagen, R.A.; Vergara, H.; Naar, D.F. Morphology of San Antonio submarine canyon on the central Chile forearc. *Mar. Geol.* **1996**, *129*, 197–205. [[CrossRef](#)]
54. Pratson, L.F.; Coakley, B.J. A model for the headward erosion of submarine canyons induced by downslope-eroding sediment flows. *GSA Bull.* **1986**, *108*, 225–234. [[CrossRef](#)]
55. Talling, P.J. How and where do incised valleys form if sea level remains above the shelf edge? *Geology* **1998**, *26*, 87–90. [[CrossRef](#)]
56. De Pippo, T.; Ilardi, M.; Pennetta, M. Main observations on genesis and morphologic evolution of submarine valleys. *Z. Geomorphol.* **1999**, *43*, 91–111. [[CrossRef](#)]
57. Brothers, T.S.; ten Brink, U.S.; Andrews, B.D.; Chaytor, J.D.; Twichell, D.C. Geomorphic process fingerprints in submarine canyons. *Mar. Geol.* **2013**, *337*, 53–66. [[CrossRef](#)]
58. Shepard, F.P.; Dill, R.F. *Submarine Canyons and Other Sea Valleys*; Rand McNally: Chicago, IL, USA, 1966; pp. 1–381.

59. Kelling, G.; Stanley, D. Sedimentation in canyon slope and base of slope environments. In *Marine Sediment Transport and Environmental Management*; Stanley, D.J., Swift, D.J.P., Eds.; Wiley: New York, NY, USA, 1976; pp. 378–435.
60. Middleton, G.V.; Hampton, M.A. Subaqueous sediment transport and deposition by sediment gravity flows. In *Marine Sediment Transport and Environmental Management*; Stanley, D.J., Swift, D.J.P., Eds.; Wiley: New York, NY, USA, 1976; pp. 197–218.
61. Sanford, M.W.; Steven, A.K.; Nittrouer, C.A. Modern sedimentary processes in the Wilmington canyon area, US east coast. *Mar. Geol.* **1990**, *92*, 51–67. [[CrossRef](#)]
62. Satterfield, W.M.; Behrens, E.W. A Late Quaternary canyon-channel system, northwest Gulf of Mexico continental slope. *Mar. Geol.* **1990**, *92*, 279–304. [[CrossRef](#)]
63. Ceramicola, S.; Amaro, T.; Amblas, D.; Cagatay, N.; Carniel, S.; Chiocci, F.L.; Fabri, M.C.; Gamberi, F.; Harris, P.; Lo Iacono, C.; et al. Submarine canyon dynamics—Executive Summary. In *Submarine Canyon Dynamics in the Mediterranean and Tributary Seas—An Integrated Geological, Oceanographic and Biological Perspective*; Briand, F., Ed.; CIESM Monograph; CIESM Publisher: Munchen, Germany, 2015; Volume 47, pp. 1–232.
64. Farre, J.A.; Mc Gregor, B.A.; Ryan, W.B.F.; Robb, J.M. Breaching the shelfbreak: Passage from youthful to mature phase in submarine canyon evolution. In *The Shelf Break: Critical Interface on Continental Margins*; Stanley, D.J., Moore, G.T., Eds.; Special Publication; Society of Economic Paleontologists and Mineralogists: Tulsa, OK, USA, 1983; Volume 33, pp. 25–39.
65. Obelcz, J.; Brothers, D.; Chaytor, J.; ten Brink, U.; Ross, S.U.; Brooke, S. Geomorphic characterization of four shelf-sourced submarine canyons along the U.S. Mid-Atlantic continental margin. *Deep Sea Res. Part II Top. Stud. Oceanogr.* **2014**, *104*, 106–119. [[CrossRef](#)]
66. Bernhardt, A.; Melnick, D.; Jara-Munoz, J.; Argandona, B.; Gonzalez, J.; Strecker, M.R. Controls on submarine canyon activity during sea-level highstands: The Biobio canyon system offshore Chile. *Geosphere* **2015**, *11*, 1226–1255. [[CrossRef](#)]
67. Nakajima, T.; Satoh, M.; Okamura, Y. Channel-levee complexes, terminal deep-sea fan and sediment wave fields associated with the Toyama Deep-Sea channel system in the Japan Sea. *Mar. Geol.* **1998**, *147*, 25–41. [[CrossRef](#)]
68. Kokelaar, P.; Romagnoli, C. Sector collapse, sedimentation and clast population evaluation of an active island-arc volcano: Stromboli, Italy. *Bull. Volcanol.* **1995**, *57*, 240–262. [[CrossRef](#)]
69. Lucchi, R.; Kidd, R.B. Sediment provenance and turbidity current processes at Lametini seamounts and Stromboli canyon. *Geomar. Lett.* **1998**, *18*, 155–164.
70. Chiocci, F.L.; Martorelli, E.; Sposato, A.; Aiello, G.; Baraza, J.; Budillon, F.; de Alteriis, G.; Ercilla, G.; Estrada, F.; Farran, M.; et al. Prime immagini TOBI del Tirreno centro-meridionale. *Geol. Romana* **1998**, *34*, 207–222.
71. Chiocci, F.L.; Tommasi, P.; Aiello, G.; Cristofalo, G.; De Lauro, M.; Tonielli, R.; Baraza, J.; Ercilla, G.; Estrada, F.; Farran, M.; et al. Submarine debris avalanche off the southern flank of Ischia volcanic island, Gulf of Naples. In Proceedings of the International Conference “Hard Soils and Soft Rocks”, Naples, Italy, 12–14 October 1998.
72. Harris, P.T.; Whiteway, T. Global distribution of large submarine canyons: Geomorphic differences between active and passive continental margins. *Mar. Geol.* **2011**, *285*, 69–86. [[CrossRef](#)]
73. Mountjoy, J.J.; Howarth, J.D.; Orpin, A.R.; Barnes, P.M.; Bowden, D.A.; Rowden, A.A.; Schimel, A.; Holden, C.; Horgan, H.; Nodder, S.; et al. Earthquakes drive large-scale submarine canyon development and sediment supply to deep-ocean basins. *Sci. Adv.* **2018**, *4*, 1–8. [[CrossRef](#)]
74. Aiello, G.; Marsella, E. The Southern Ischia canyon system: Examples of deep sea depositional systems on the continental slope off Campania (Italy). *Rend. Online Della Soc. Geol. Ital.* **2014**, *32*, 28–37. [[CrossRef](#)]
75. Deino, A.L.; Orsi, G.; De Vita, S.; Piochi, M. The age of the Neapolitan Yellow Tuff caldera-forming eruption (Campi Flegrei caldera—Italy) assessed by $^{40}\text{Ar}/^{39}\text{Ar}$ dating method. *J. Volcanol. Geotherm. Res.* **2004**, *133*, 157–170. [[CrossRef](#)]
76. Aiello, G.; Insinga, D.D.; Iorio, M.; Meo, A.; Senatore, M.R. On the occurrence of the Neapolitan Yellow Tuff tephra in the Northern Phlegrean Fields offshore (Eastern Tyrrhenian margin, Italy). *Ital. J. Geosci.* **2017**, *136*, 263–274. [[CrossRef](#)]
77. Milia, A. The Dohrn canyon: A response to the eustatic fall and tectonic uplift of the outer shelf along the eastern Tyrrhenian sea margin, Italy. *Geomar. Lett.* **2000**, *20*, 101–108. [[CrossRef](#)]

78. D'Argenio, B.; Aiello, G.; de Alteriis, G.; Milia, A.; Sacchi, M.; Tonielli, R.; Budillon, F.; Chiocci, F.L.; Conforti, A.; De Lauro, M.; et al. Digital Elevation Model of the Naples Bay and adjacent areas, Eastern Tyrrhenian sea. In *Mapping Geology in Italy*; Groppelli, G., Goette, V., Eds.; Editore De Agostini: Rome, Italy, 2004; pp. 1–8.
79. Di Fiore, V.; Aiello, G.; D'Argenio, B. Gravity instabilities in the Dohrn canyon (Bay of Naples, Southern Tyrrhenian sea): Potential wave and run-up (tsunami) reconstruction from a fossil submarine landslide. *Geol. Carpath.* **2011**, *62*, 55–63. [[CrossRef](#)]
80. Budillon, F.; Cesarano, M.; Insinga, D.D.; Pappone, G. Activation versus de-activation of a Pleistocene turbidite system in response to major volcanic events: The example of the Dohrn canyon-fan system in the continental slope off the Campania region (Southern Tyrrhenian sea, Italy). *Rend. Online Della Soc. Geol. Ital.* **2016**, *40* (Suppl. 1), 595.
81. Passaro, S.; Tamburrino, S.; Vallefucio, M.; Gherardi, S.; Sacchi, M.; Ventura, G. High-resolution morpho-bathymetry of the Gulf of Naples, Eastern Tyrrhenian sea. *J. Maps* **2016**, *12*, 203–210. [[CrossRef](#)]
82. Taviani, M.; Angeletti, L.; Cardone, F.; Montagna, P.; Danovaro, R. A unique and threatened deep water coral-bivalve biotope new to the Mediterranean Sea offshore the Naples megalopolis. *Sci. Rep.* **2019**, *9*, 3411. [[CrossRef](#)]
83. International Hydrographic Organization (IHO). *IHO Standards for Hydrographic Surveys*, 5th ed.; Special Publication 44; The International Hydrographic Bureau: Monte Carlo, Monaco, 2008; pp. 1–28.
84. Amadio, G. La cartografia in forma raster. *Boll. Geod. Sci. Affin.* **1992**, *51*, 227–242.
85. Mitchum, R.M.; Vail, P.R.; Sangree, J.B. Stratigraphic interpretation of seismic reflection patterns in depositional sequences. In *Seismic Stratigraphy—Applications to Hydrocarbon Exploration*; Payton, C.E., Ed.; AAPG Mem: Tulsa, OK, USA, 1977; Volume 26, pp. 117–133.
86. Vail, P.R.; Mitchum, R.M.; Thompson, S. Relative changes of sea level from coastal onlap. In *Seismic Stratigraphy—Applications to Hydrocarbon Exploration*; Payton, C.E., Ed.; AAPG Mem: Tulsa, OK, USA, 1977; Volume 26, pp. 63–81.
87. Anstey, N.A. *Simple Seismics*; International Human Resources Development and Co.: Boston, MA, USA, 1982.
88. Mitchum, R.M. Seismic stratigraphy and global changes in sea level, part II Glossary of terms used in seismic stratigraphy. In *Seismic Stratigraphy—Applications to Hydrocarbon Exploration*; Payton, C.E., Ed.; AAPG Mem: Tulsa, OK, USA, 1977; Volume 26, pp. 205–212.
89. Vail, P.R.; Mitchum, R.M.; Thompson, S. Global cycles of relative changes of sea level. In *Seismic Stratigraphy—Applications to Hydrocarbon Exploration*; Payton, C.E., Ed.; AAPG Mem: Tulsa, OK, USA, 1977; Volume 26, pp. 83–97.
90. Vail, P.R.; Todd, R.G.; Sangree, J.B. Chronostratigraphic significance of seismic reflections. In *Seismic Stratigraphy—Applications to Hydrocarbon Exploration*; Payton, C.E., Ed.; AAPG Mem: Tulsa, OK, USA, 1977; Volume 26, pp. 99–116.
91. Vail, P.R.; Hardenbol, J.; Todd, R.G. Jurassic unconformities, chronostratigraphy and sea-level changes from seismic stratigraphy and biostratigraphy. In *Interregional Unconformities and Hydrocarbon Accumulation*; Schlee, J.S., Ed.; AAPG Mem: Tulsa, OK, USA, 1977; Volume 36, pp. 129–144.
92. Roksandic, M.M. Seismic facies analysis concepts. *Geophys. Prospect.* **1978**, *26*, 383–398. [[CrossRef](#)]
93. Dumay, J.; Fournier, F. Multivariate statistical analyses applied to seismic facies recognition. *Geophysics* **1988**, *53*, 1151–1159. [[CrossRef](#)]
94. West, B.P.; May, S.R.; Eastwood, J.E.; Rossen, C. Interactive seismic facies classification using textural attributes and neural networks. *Lead. Edge* **2002**, *21*, 1042–1049. [[CrossRef](#)]
95. De Matos, M.C.; Osorio, P.; Johann, P. Unsupervised seismic facies analysis using wavelet transform and self-organizing maps. *Geophysics* **2007**, *72*, P9–P21. [[CrossRef](#)]
96. Marroquin, I.; Brault, J.; Hart, B. A visual data mining methodology for seismic facies analysis—Part I—Testing and comparison with other unsupervised clustering methods. *Geophysics* **2009**, *74*, P1–P11. [[CrossRef](#)]
97. Folk, R.L.; Ward, W.C. Brazos River bar [Texas]; a study in the significance of grain size parameters. *J. Sediment. Res.* **1957**, *27*, 3–26. [[CrossRef](#)]
98. Malinverno, A. Evolution of the Tyrrhenian Sea-Calabrian Arc system: The past and the present. *Rendiconti Online Della Soc. Geol. Ital.* **2012**, *21*, 11–15.

99. Doglioni, C. A proposal for kinematic modeling for W-dipping subductions—Possible applications to the Tyrrhenian-Apennines system. *Terra Nova* **1991**, *3*, 423–434. [[CrossRef](#)]
100. Gueguen, E.; Doglioni, C.; Fernandez, M. On the post-25 Ma geodynamic evolution of the western Mediterranean. *Tectonophysics* **1998**, *298*, 259–269. [[CrossRef](#)]
101. Rosenbaum, G.; Lister, G.S. Neogene and Quaternary rollback evolution of the Tyrrhenian sea, the Apennines, and the Sicilian Maghrebides. *Tectonics* **2004**, *23*. [[CrossRef](#)]
102. Mattei, M.; Cifelli, F.; D’Agostino, N. The evolution of the Calabrian arc: Evidence from paleomagnetic and GPS observations. *Earth Planet. Sci. Lett.* **2007**, *263*, 259–274. [[CrossRef](#)]
103. Patacca, E.; Scandone, P. Geology of the Southern Apennines. *Boll. Della Soc. Geol. Ital.* **2007**, *7*, 75–119.
104. Knott, S.D. Structure, kinematics and metamorphism in the Liguride Complex, Southern Apennines, Italy. *J. Struct. Geol.* **1994**, *16*, 1107–1120. [[CrossRef](#)]
105. Cello, G.; Mazzoli, S. Apennine tectonics in Southern Italy: A review. *J. Geodyn.* **1999**, *16*, 191–211. [[CrossRef](#)]
106. Ippolito, F.; Ortolani, F.; Russo, M. Struttura marginale tirrenica dell’Appennino campano: Reinterpretazioni di dati di antiche ricerche di idrocarburi. *Mem. Della Soc. Geol. Ital.* **1973**, *12*, 227–250.
107. Cinque, A.; Aucelli, P.P.C.; Brancaccio, L.; Mele, R.; Milia, A.; Robustelli, G.; Romano, P.; Russo, F.; Russo, M.; Santangelo, N.; et al. Volcanism, tectonics and recent geomorphological change in the Bay of Napoli. *Suppl. Geogr. Fis. Din. Quat.* **1997**, *3*, 123–141.
108. Mariani, M.; Prato, R. I bacini neogenici costieri del margine tirrenico: Approccio sismico-stratigrafico. *Mem. Della Soc. Geol. Ital.* **1988**, *41*, 519–531.
109. Brancaccio, L.; Cinque, A.; Romano, P.; Russo, F.; Santangelo, N.; Santo, A. Geomorphology and neotectonic evolution of a sector of a Tyrrhenian flank of the southern Apennines (Region of Naples, Italy). *Zeitsch Geomorphol.* **1991**, *82*, 47–58.
110. Milia, A.; Torrente, M.M.; Russo, M.; Zuppetta, A. Tectonics and crustal structure of the Campania continental margin: Relationships with volcanism. *Mineral. Petrol.* **2003**, *79*, 33–47. [[CrossRef](#)]
111. Turco, E.; Schettino, A.; Pierantoni, P.P.; Santarelli, G. The Pleistocene extension of the Campania Plain in the framework of the southern Tyrrhenian tectonic evolution. In *Volcanism in the Campania Plain: Vesuvius, Campi Flegrei and Ignimbrites*; De Vivo, B., Ed.; Developments in Volcanology; Elsevier: Amsterdam, The Netherlands, 2006; Volume 9, pp. 27–51.
112. Santangelo, N.; Romano, P.; Ascione, A.; Russo Ermolli, E. Quaternary evolution of the Southern Apennines coastal plains: A review. *Geol. Carpathica* **2017**, *68*, 1–43. [[CrossRef](#)]
113. Aiello, G.; Marsella, E.; Cicchella, A.G.; Di Fiore, V. New insights on morpho-structures and seismic stratigraphy along the Campania continental margin (Southern Italy) based on deep multichannel seismic profiles. *Rend. Lincei* **2011**, *22*, 349–373. [[CrossRef](#)]
114. Aiello, G.; Marsella, E. Interactions between late Quaternary volcanic and sedimentary processes in the Naples Bay, southern Tyrrhenian sea. *Ital. J. Geosci.* **2015**, *134*, 367–382. [[CrossRef](#)]
115. Armenti, P.; Barberi, F.; Birounard, H.; Clocchiatti, R.; Innocenti, F.; Metrich, N.; Rosi, M. The Phlegrean Fields: Magma evolution within a shallow chamber. *J. Volcanol. Geotherm. Res.* **1983**, *17*, 289–312. [[CrossRef](#)]
116. Rosi, M.; Sbrana, A.; Principe, C. The Phlegrean Fields: Structural evolution, volcanic history and eruptive mechanisms. *J. Volcanol. Geotherm. Res.* **1983**, *17*, 273–288. [[CrossRef](#)]
117. Judenherc, S.; Zollo, A. The Bay of Naples (Southern Italy): Constraints on the volcanic structures inferred from a dense seismic survey. *J. Geophys. Res.* **2004**, *B10312*, 109. [[CrossRef](#)]
118. Berrino, G.; Corrado, G.; Riccardi, U. Sea gravity in the Gulf of Naples. A contribution to delineating the structural pattern of Phlegraean Volcanic District. *J. Volcanol. Geotherm. Res.* **2008**, *175*, 241–252. [[CrossRef](#)]
119. Zollo, A.; Maercklin, N.; Vassallo, M.; Dello Iacono, D.; Virieux, J.; Gasparini, P. Seismic reflections reveal a massive melt layer feeding Campi Flegrei caldera. *Geophys. Res. Lett.* **2008**, *35*, L12306. [[CrossRef](#)]
120. De Natale, G.; Troise, C.; Darren, M.; Mormone, A.; Piochi, M.; Di Vito, M.A.; Isaia, R.; Carlino, S.; Barra, D.; Somma, R. The Campi Flegrei Deep Drilling Project (CFDDP): New insight on caldera structure, evolution and hazard implications for the Naples area (Southern Italy). *Geochem. Geophys. Geosyst.* **2016**, *17*, 4836–4847. [[CrossRef](#)]
121. Torrente, M.M.; Milia, A. Comment on “The Campi Flegrei Deep Drilling Project (CFDDP): New Insight on Caldera Structure, Evolution and Hazard Implications for the Naples Area (Southern Italy) by G. De Natale et al. *Geochem. Geophys. Geosyst.* **2018**, *19*, 2283–2288. [[CrossRef](#)]

122. Aiello, G. Techniques and methods of seismic data processing in active volcanic areas: Some applications to multichannel seismic profiles (Gulf of Naples, Southern Tyrrhenian sea, Italy). *J. Geogr. Cartogr.* **2019**, *1*, 1–24.
123. Rolandi, G.; Bellucci, F.; Heizler, M.T.; Belkin, H.E.; De Vivo, B. Tectonic controls on the genesis of ignimbrites from the Campanian Volcanic Zone, southern Italy. *Mineral. Petrol.* **2003**, *79*, 3–31. [[CrossRef](#)]
124. Bellucci, F.; Milia, A.; Rolandi, G.; Torrente, M.M. Chapter 8: Structural control on the Upper Pleistocene ignimbrite eruptions in the Neapolitan area (Italy): Volcano-tectonic faults versus caldera faults. In *Volcanism in the Campania Plain: Vesuvius, Campi Flegrei and Ignimbrites*; De Vivo, B., Ed.; Developments in Volcanology; Elsevier: Amsterdam, The Netherlands, 2006; Volume 9, pp. 163–180.
125. Milia, A.; Torrente, M.M. The influence of paleogeographic setting and crustal subsidence on the architectures of ignimbrites in the Bay of Naples (Italy). *Earth Planet. Sci. Lett.* **2007**, *263*, 192–206. [[CrossRef](#)]
126. Ascione, A.; Romano, P. Vertical movements on the eastern margin of the Tyrrhenian extensional basin. New data from Mt. Bulgheria (Southern Apennines, Italy). *Tectonophysics* **1999**, *315*, 337–356. [[CrossRef](#)]
127. Fusi, N.; Mirabile, L.; Camerlenghi, A.; Ranieri, G. Marine geophysical survey of the Gulf of Naples (Italy): Relationships between submarine volcanic activity and sedimentation. *Mem. Della Soc. Geol. Ital.* **1991**, *47*, 95–114.
128. Torrente, M.M.; Milia, A.; Bellucci, F.; Rolandi, G. Extensional tectonics in the Campania Volcanic Zone (eastern Tyrrhenian sea, Italy): New insights into the relationship between faulting and ignimbrite eruptions. *Ital. J. Geosci.* **2010**, *129*, 297–315.
129. Di Girolamo, P. Petrografia dei tufi Campani: Il processo di pipernizzazione (Tufo-Tufo pipernoide-Piperno). *Rend. Accad. Sci. Fis. Mat. Napoli* **1968**, *5*, 4–25.
130. De Vivo, B.; Rolandi, G.; Gans, P.B.; Calvert, A.; Bohron, W.A.; Spera, J.; Belkin, H.E. New constraints on the pyroclastic eruptive history of the Campanian volcanic Plain (Italy). *Miner. Petrol.* **2001**, *73*, 47–65. [[CrossRef](#)]
131. Deino, A.L.; Curtis, G.H.; Rosi, M. $^{40}\text{Ar}/^{39}\text{Ar}$ dating of the Campanian Ignimbrite, Campanian Region. In Proceedings of the 29th International Geological Congress, Kyoto, Japan, 24 August–3 September 1992; Volume 3, p. 2654.
132. Deino, A.L.; Curtis, G.H.; Southon, I.; Terrasi, F.; Campajola, L.; Orsi, G. ^{14}C and $^{40}\text{Ar}/^{39}\text{Ar}$ dating of the Campanian Ignimbrite, Phlegrean Fields, Italy. In Proceedings of the International Conference on Geochronology, Berkeley, CA, USA, 5–11 June 1994; pp. 1–77.
133. Giaccio, B.; Hajdas, I.; Isaia, R.; Deino, A.; Nomade, S. High precision ^{14}C and $^{40}\text{Ar}/^{39}\text{Ar}$ dating of the Campanian Ignimbrite (Y-5) reconciles the time-scales of climatic-cultural processes at 40 ka. *Sci. Rep.* **2017**, *7*, 45940. [[CrossRef](#)]
134. Romano, P.; Santo, A.; Voltaggio, M. L'evoluzione geomorfologica della pianura del fiume Volturno (Campania) durante il tardo Quaternario (Pleistocene medio-superiore/Olocene). *Il Quat.* **1994**, *7*, 41–56.
135. Bellucci, F. Nuove conoscenze stratigrafiche sui depositi vulcanici del sottosuolo del settore meridionale della Piana Campana. *Boll. Della Soc. Geol. Ital.* **1994**, *113*, 395–420.
136. Aiello, G.; Marsella, E.; Giordano, L.; Passaro, S. Seismic stratigraphy and marine magnetics in the Naples Bay (Southern Tyrrhenian sea): The onset of new technologies and methodologies for data acquisition, processing and interpretation. In *Stratigraphic Analysis of Layered Deposits*; Intech Science Publishers: Rijeka, Croatia, 2012; pp. 21–60.
137. Passaro, S.; Tamburrino, S.; Vallefuoco, M.; Tassi, F.; Vaselli, O.; Giannini, L.; Chiodini, G.; Caliro, S.; Sacchi, M.; Rizzo, A.L.; et al. Seafloor doming driven by degassing processes unveils sprouting volcanism in coastal areas. *Sci. Rep.* **2016**, *6*, 22448. [[CrossRef](#)]
138. Aiello, G.; Budillon, F.; Cristofalo, G.; D'Argenio, B.; de Alteriis, G.; De Lauro, M.; Ferraro, L.; Marsella, E.; Pelosi, N.; Sacchi, M.; et al. Marine geology and morphobathymetry in the Bay of Naples. In *Structures and Processes of Mediterranean Ecosystems*; Springer: Milano, Italy, 2001; pp. 1–8.
139. Aiello, G.; Cicchella, A.G. Dati sismostratigrafici sul margine continentale della Campania tra Ischia, Capri ed il bacino del Volturno (Tirreno meridionale, Italia) in base al processing sismico ed all'interpretazione geologica di profili sismici a riflessione multicanale. *Quad. Geofis.* **2019**, *149*, 1–52.
140. Passaro, S.; Sacchi, M.; Tamburrino, S.; Ventura, G. Fluid Vents, Flank Instability, and Seafloor Processes along the Submarine Slopes of the Somma-Vesuvius Volcano, Eastern Tyrrhenian Margin. *Geosciences* **2018**, *8*, 60. [[CrossRef](#)]

141. Sacchi, M.; De Natale, G.; Spiess, V.; Steinmann, L.; Acocella, V.; Corradino, M.; de Silva, S.; Fedele, A.; Fedele, L.; Geshi, N.; et al. A roadmap for amphibious drilling at the Campi Flegrei caldera: Insights from a MagellanPlus workshop. *Sci. Drill.* **2019**, *7*, 1–18. [[CrossRef](#)]
142. Aiello, G.; Marsella, E.; Passaro, S. Submarine instability processes on the continental slopes off the Campania region (Southern Tyrrhenian sea, Italy): The case history of Ischia island (Naples Bay). *Boll. Geofis. Teor. Appl.* **2009**, *50*, 193–207.
143. Ricci Lucchi, F. *Sedimentologia*; CLUEB: Bologna, Italy, 1972; Volume I, pp. 1–217.
144. Chiocci, F.L.; Orlando, L.; Tortora, P. Small-scale seismic stratigraphy and paleogeographical evolution of the continental shelf facing the SE Elba island (Northern Tyrrhenian Sea, Italy). *J. Sediment. Petrol.* **1991**, *61*, 506–526.
145. Druckman, Y.; Buchbinder, B.; Martinotti, G.M.; Siman Tov, R.; Aharon, P. The buried Afiq canyon (eastern Mediterranean, Israel): A case study of a Tertiary submarine canyon exposed in Late Messinian times. *Mar. Geol.* **1995**, *123*, 167–185. [[CrossRef](#)]
146. Hernandez-Molina, F.; Somoza, L.; Lobo, F. Seismic stratigraphy of the Gulf of Cadiz continental shelf. A model for Late Quaternary very high resolution sequence stratigraphy and response to sea level fall. *Geol. Soc. Lond. Spec. Publ.* **2000**, *172*, 329–362. [[CrossRef](#)]
147. Lericolais, G.; Auffret, M.; Bourillet, J.F. The Quaternary Channel River: Seismic stratigraphy of its palaeo-valleys and deepes. *J. Quat. Sci.* **2003**, *18*, 245–260. [[CrossRef](#)]
148. Bourillet, F.; Zaragosi, S.; Mulder, T. The French Atlantic margin and deep sea submarine systems. *Geomarine Lett.* **2006**, *26*, 311–315. [[CrossRef](#)]
149. Gupta, S.; Collier, J.S.; Felgate, A.P.; Potter, G. Catastrophic flooding origin of shelf valley systems in the English Channel. *Nature* **2007**, *448*, 342–345. [[CrossRef](#)]
150. Toucanne, S.; Zaragosi, S.; Bourillet, J.F.; Marieu, V.; Cremer, M.; Kageyama, M.; Van Vliet Lanoe, B.; Eynaud, F.; Turon, J.L.; Gibbard, P.L. The first estimation of Fleuve Manche palaeoriver discharge during the last deglaciation: Evidence for Fennoscandian ice sheet meltwater flow in the English Channel ca 20–18 ka ago. *Earth Planet. Sci. Lett.* **2010**, *290*, 459–473. [[CrossRef](#)]
151. Fusi, N. Structural setting of the carbonatic basement and its relationship with the magma uprising in the Gulf of Naples (Southern Italy). *Ann. Geophys.* **1996**, *39*, 493–509.
152. Mirabile, L.; De Marinis, E.; Frattini, M. The Phlegrean fields beneath the sea: The underwater volcanic district of Naples, Italy. *Boll. Geofis. Teor. Appl.* **2000**, *41*, 159–186.



© 2020 by the authors. Licensee MDPI, Basel, Switzerland. This article is an open access article distributed under the terms and conditions of the Creative Commons Attribution (CC BY) license (<http://creativecommons.org/licenses/by/4.0/>).